# Sedimentary Architecture of an Ancient Linear Megadune (Barremian, Neuquén Basin): Insights into the Long-Term Development and Evolution of Aeolian Linear Bedforms

**AGUSTÍN ARGÜELLO SCOTTI[1*] and GONZALO D. VEIGA[1]**

*[1]Centro de Investigaciones Geológicas (CONICET-Universidad Nacional de La Plata), Diagonal 113 #275 (B1904DPK), La Plata, Argentina.*

**Corresponding author (e-mail address: aarguello@cig.museo.unlp.edu.ar )*

**Present address: YPF S.A., Macacha Guemes #515 (C1106BKK), Ciudad Autónoma de Buenos Aires, Argentina.*

**Short title: Architecture of Aeolian Linear Bedforms**

## ABSTRACT

Linear aeolian bedforms are the most abundant bedform type in modern Earth sand seas and are very common in our Solar System. Despite their abundance, the long-term development of these bedforms and its impact upon the resulting sedimentary architecture in the geological record is still poorly understood. The aims of this paper are to study the exposed record of an ancient linear megadune in order to discuss the factors that impact the development and sedimentary architecture of aeolian linear bedforms. The outcrops of the ancient Troncoso Sand Sea (Barremian, Neuquén Basin, Argentina) provide a unique opportunity to access a preserved megadune record with an external body geometry that unequivocally confirms its linear morphology. Architectural analysis of the bedform record reveals significant differences for several aspects of cross-stratified set bodies and bounding surfaces and allows for the identification of three architectural complexes. Insights from deterministic models, analysis of set body relative chronology and distribution suggest that complexes result from distinctive phases in bedform development. It also clearly shows that the megadune's construction was achieved by expansion from a core, where the oldest deposits are located, and that its development was characterized by sustained growth and strong longitudinal dynamics. Factors that impact the development and architecture of linear bedforms are identified, discussed, and compared to bedforms of transverse dynamics. Finally, a scheme of expected styles of sedimentary architecture for linear bedforms is presented. This case study shows how growth can be a critical factor conditioning linear bedform architecture and indicates how the preservation of certain styles of sedimentary architecture in the geological record may not be as unusual as previously thought.


**Keywords: sedimentary architecture, aeolian linear bedforms, bedform development, Cretaceous, Neuquén Basin, Troncoso Inferior**

## INTRODUCTION

Linear dunes -relatively symmetric, continuous, simple forms- (Lancaster, 1995; Livingstone and Warren, 1996) and linear megadunes -dunes with superimposed dunes- (also known as *draa;* Wilson, 1972; Mountney, 2006) are the most abundant bedform type in modern sandy deserts (Lancaster, 1982). In spite of this, establishing the dominant characteristics of the sedimentary architecture associated with these bedforms has been problematic over several decades (Rodríguez-López *et al.,* 2014; Besly *et al.,* 2018). The difficulty to access the interior of modern dunes (McKee and Tibbitts, 1964; Tsoar, 1982), the apparent scarcity of this dune type in the geological record (Rubin and Hunter, 1985), and open questions about the long-term behaviour of these particularly slow-moving bedforms (Rubin *et al.*, 2008), have made it difficult to record, predict and identify the sedimentary architecture resulting from linear bedform development.

In this study, the term "linear" is used strictly to refer to bedform morphology, following Rubin and Hunter (1985). Dunes of linear morphology include a variety of scales and shapes, such as *seifs* (Bagnold, 1941; Tsoar, 1982; Lancaster, 1995), linear ridges (vegetated linear dunes of Tsoar, 1989; Warren, 2013) and complex or compound (McKee, 1979) linear megadunes. Linear bedforms can also be classified according to their dynamics in longitudinal or oblique (*sensu* Rubin and Hunter, 1985), which result from the relative importance of elongation (*sensu* Tsoar *et al.*, 2004) and lateral migration (Bristow *et al.*, 2005; Rubin *et al.*, 2008) processes.

Relatively recently, GPR and OSL techniques on modern dunes have allowed the characterization of simple linear dune's sedimentary architecture and have improved our understanding of their dynamics (Bristow *et al.*, 2000, 2007; Roskin *et al.*, 2011). However, long-term variability in linear bedform dynamics, scale and shape, and their effect on the sedimentary architecture preserved in the geological record, are still poorly understood.

Considering that GPR studies of recent dunes have spatial limitations (e.g. imaging penetration depth), the study of outcrop analogues offers a great opportunity to test models of sedimentary architecture attributed to linear bedforms, especially regarding larger megadune-scale forms, and to obtain further insights regarding their long-term development.

In the geological record, most examples of sedimentary deposits assigned to deposition by linear bedforms seem to fall between two types of sedimentary architecture (Fig. 1). These are commonly referred to as "lateral migration" and "vertical accretion" models, given their interpreted association with bedform dynamics (Rubin and Hunter 1985; Clemmensen, 1989; Scherer, 2000). Examples from the former category are broadly characterized by unimodal spread of cross-stratification dip-azimuths, oblique to the dip-azimuths of the internal bounding surfaces (Clemmensen, 1989; Ahmed Benan and Kocurek, 2000; Scherer, 2000; Rodríguez-López *et al.*, 2008; Besly *et al.*, 2018), and are consistent with lateral migration-dominated theoretical models proposed by Rubin and Hunter (1985). Other ancient examples fall within the latter category and are characterized by a bimodal (not bipolar) distribution of cross-stratification dip-azimuths (Glennie, 1972; Steele, 1983; Clemmensen, 1989; Bose *et al.*, 1999), and are consistent with longitudinal behaviour theoretical models proposed by Rubin and Hunter (1985). Nonetheless, ancient examples with good exposures across a preserved bedform with an external geometry that clearly confirms its linear morphology are very few in number (Clemmensen, 1989; Scherer, 2000).

The aeolian deposits within the Troncoso Inferior Member of the Huitrín Formation (Neuquén Basin, Argentina) are characterized by the exceptional preservation of large- and small-scale bedform morphology (Veiga *et al.*, 2005). Large-scale bedforms of linear morphology have been identified in this ancient aeolian system both in remarkable quality exposures (Strömbäck *et al.*, 2005; Argüello Scotti and Veiga, 2015) and in the subsurface (Dajczgewand *et al.*, 2006). The aims of this work are to study the sedimentary architecture

within an exceptionally preserved and exposed linear megadune from the geological record of the Troncoso Inferior Member, obtain a conceptual model of its development, and discuss the factors that impact the development and sedimentary architecture of linear aeolian bedforms.

## GEOLOGICAL SETTING AND STUDY AREA

The Troncoso Inferior Member of the Huitrín Formation (Groeber, 1946) is part of the sedimentary infill of the Neuquén Basin (Howell *et al.*, 2005) (Fig. 2). It is considered to be Barremian in age, constrained by fossil assemblages in underlying and overlying marine units (Lazo and Damborenea, 2011; Aguirre-Urreta *et al.*, 2017). In the north-eastern sector of the basin, the study unit is characterized by sandstones related to the development of a large dune field or *erg*, overlying sandstones of fluvial/aeolian origin or, in some cases, a variety of sedimentary deposits of marine origin. This *erg*, known as the Troncoso Sand Sea (Argüello Scotti, 2017), has a preserved extension of over 6000 $km^2$ and was developed during a period when the basin was completely disconnected from the proto-Pacific Ocean, being therefore considered as an inland *erg*. The final morphology of the dune field is partially preserved due to the abrupt marine flooding of the basin and the subsequent deposition of evaporites, due to a partial reconnection with the open ocean (Veiga *et al.*, 2005).

The area selected for this study is the Loma La Torre outcrop at the southern Pampa de Tril plain, in the north-western Neuquén Province (Figs. 2, 3). Previous studies in this location show that large-scale sandstone ridges that characterize the uppermost interval of the study unit constitute exceptionally preserved linear-shaped bedforms (Strömbäck *et al.*, 2005; Veiga *et al*., 2005). These ridges are oriented WSW-ENE and have a width close to 1 km, a symmetric cross-section, a spacing close to 1.5 km, and a preserved remnant height of 24-30 m (Argüello Scotti and Veiga, 2015). The *erg* system's record, which constitutes the study interval, is bounded at the base by a planar and subhorizontal sand-drift surface (*sensu*

Clemmensen and Tirsgaard, 1990; Rodríguez-López *et al.*, 2013), characterized by signs of deflation, and capped at the top by a marine transgressive super surface (*sensu* Havholm and Kocurek, 1994). This interval regularly thins out in the so-called "interdune sectors", as the two previously mentioned surfaces merge, indicating that the Troncoso Sand Sea record in this locality comprises solely the record of the preserved large-scale bedforms. When the system record thickness drops below one metre, interdune facies can be observed which lack indication of water-lain, or even water-influenced, deposition. According to the facies observed in the interdune sectors, the aeolian system in the study area can be classified as dry (*sensu* Kocurek and Havholm, 1993). Furthermore, the very low or null thickness of the system's record in the interdune indicate the absence of a rise in the accumulation surface, confirming that the system did not undergo accumulation (*sensu* Kocurek, 1999). Finally, considering regional studies (Fig. 2), the system at the study area was most likely located in a marginal *erg* setting.

The most accessible large-scale preserved bedform at the Loma La Torre outcrop was selected for this study (Fig. 3). Additional information on the preserved morphology and thickness of the bedform's record are available from a previous study (Argüello Scotti and Veiga, 2015). The outcrops of the preserved bedform´s record comprise a continuous two-dimensional cliff section of its southern flank, oriented N110°-290° and oblique to bedform orientation (N81°-261°), and a discontinuous but more pseudo three-dimensional exposure of its northern flank.

Previous facies analysis of the study interval at this locality (Veiga *et al*., 2005; Argüello Scotti and Veiga, 2015) recognized a low variability of sedimentary facies, belonging to aeolian and subordinated soft-sediment deformed facies associations. The most abundant facies are well to moderately sorted, fine- to medium-grained, cross-stratified sandstones. Cross-stratification can be of both trough and planar type, and from high to low dip angle.

More rarely, subhorizontally bedded sandstones occur (Fig. 4A, B). Basic aeolian stratification types characteristic of deposition in a dry sandy substrate are abundant (grainfall laminae, grainflow strata, subcritically climbing translatent strata; Fig. 4B, C, D), while stratification types indicating deposition under a damp surface (adhesion ripple forms) have only been found in one sector of the preserved large-scale bedform core (and not in the interdune). Soft-sediment deformation of aeolian facies is evidenced by structures distorting primary aeolian strata by folding, such as convolute laminae, wavy subparallel bedding, cone-shaped diapirs and broad synclines, and by dish structures. These facies are only abundant in the upper sectors of the study interval, and have been associated to rapid upwards escape of water and/or air associated with pressure changes within the dunes resulting from flooding (Strömbäck *et al.*, 2005).

## METHODS

The workflow designed for this study is centred on a sedimentary architecture analysis (Kocurek *et al.*, 1991). Field data acquisition (qualitative and quantitative) focused on two key elements of the sedimentary record of the preserved bedform: the cross-stratified set bodies and their bounding surfaces. Characterization of these elements allowed for the definition of contrasting architectural styles, identified as “architectural complexes”, whose internal complexity, distribution and chronology of set bodies was analysed.

### Data acquisition and processing

A combination of surveying methods was used to characterize the sedimentary architecture exposed in the outcrops, including (i) ground- and aerial-based photography, (ii) sedimentary logs, and (iii) direct measurements and observations over the accessible parts of the outcrop.

Aerial photography was used to build a digital photomosaic over which the inferred sedimentary architecture was mapped, and later confirmed or corrected with field observations, resulting in three architectural panels. From these panels, the shape and position of the individual cross-stratified bodies and bounding surfaces were analysed. The position of each element was established in relation to the morphological features observed in the study section, such as megadune flank and crest sectors (Fig. 3D). Six detailed sedimentary logs were measured across the study section (Fig. 5), allowing for grain-size and sorting inspection (using a magnifying lens and comparative charts) aeolian stratification types recognition and estimation of their abundance within set bodies, set body thickness measurements, and dip angle and azimuth readings of cross-stratification and bounding surfaces using a Brunton compass. Direct measurements and observations were carried out for all set bodies and intervening bounding surfaces that were accessible by foot, delivering the same information as logs. Specific categories were defined to estimate the relative abundance of aeolian stratification types within set bodies. Criteria used for recognition of aeolian stratification types are the same as in Argüello Scotti and Veiga (2015). The following categories were identified from the relative abundance between wind-ripple laminae (climbing translatent strata of Hunter, 1977) and grainflow strata (Kocurek and Dott, 1981): (i) wind-ripple dominated (no grainflow); (ii) wind-ripple abundant; (iii) wind-ripple/grainflow couplets; (iv) grainflow abundant; (v) grainflow-dominated (no wind-ripple). Grainfall laminae were identified and usually present at all these categories, but they were of little volumetric importance in the section and across the study interval in general. Finally, a virtual outcrop model was generated from ground- and aerial-based photography, following a structure-from-motion workflow. The model was built from approximately 200 photographs, using Visual SFM (Wu, 2011) and MeshLab (Cignoni *et al.*, 2008) software, and was scaled and referenced with data from a total station survey. The model was then imported into

Virtual Reality Geological Studio (Hodgetts, 2009; Rarity *et al.,* 2014), where cross-stratified set body dimensions (maximum thickness and apparent width) were obtained with vertical and horizontal measuring tools, and additional measurements of dip angle and azimuth of cross-stratification and bounding surfaces were extracted with the dip-azimuth tool (that calculates dip-azimuth from three points manually picked in the model). The final architectural panels (Fig. 6) combine the information obtained from all these sources.

As a result, a total of 70 cross-stratified set bodies were analysed for the preserved bedform studied. The final dataset includes a total of 137 dip-azimuth readings of cross-stratification from 46 set bodies, and a total of 37 dip-azimuth readings from bounding surfaces. Dip-azimuth cross-stratification measurements were averaged for each set body, resulting in what is here referred to as "palaeocurrent direction". In addition, the intra-body variability of cross-stratification dip-azimuth was measured as a strength vector (Collinson *et al.*, 2006) when at least 3 values per body were available.

**Data analysis**

The architectural complexes identified within the study section are defined by significant differences in several aspects of the set bodies and bounding surfaces, such as maximum thickness, apparent width, palaeocurrent and bounding surface orientations and external geometry (Figs. 6, 7, Table 1, 2). Minor differences are also seen in the abundance of aeolian stratification types and textural and compositional aspects of the sandstones. Statistically significant differences were found between the maximum thickness of set bodies belonging to different complexes by Fisher's variance test (ANOVA) at a level of $p<0.05$ [$F(3.64) = 23.36$; $p<0.0001$], and by Kruskal-Wallis test also at $p<0.05$ [$H = 40.85$; $p<0.0001$]. Very similarly, significant differences of apparent width measurements of set bodies were established by Fisher's variance test (ANOVA) [$F(3.48) = 20.25$; $p<0.0001$] and Kruskal-

Wallis test [H = 34.79; p<0.0001], always at a level of $p<0.05$. Tukey's and Dunn's tests for multiple comparisons (Table 2) indicated the specific differences between each population. Reconstruction and interpretation of the bedform morphodynamics and development that relate to each complex was assisted by deterministic modelling using BEDFORMS software (Rubin, 1987). In addition, the distribution of the complexes (i.e., location within the study section, abundance and relative superposition) and the internal relative chronology of their set bodies was inspected. These analyses provided a wealth of information that allowed reconstructing the development of this ancient linear megadune.

## SEDIMENTARY ARCHITECTURE

### Architectural complexes

The sedimentary architecture observed in the study section is separated into three complexes with particular architectural styles (Figs. 6, 7, Tables 1, 2). The architectural style is considered in terms of the dimensions, shape and distribution of set bodies and orientation of both foresets and bounding surfaces. The differences between complexes (quantitative and qualitative) are demonstrated to be the result of a particular phase in the development of the preserved bedform, indicating that each complex is composed of genetically-related set bodies and bounding surfaces.

#### *Complex 1*

*Description.* Complex 1 is characterized by small cross-stratified set bodies (maximum thickness usually between 1 and 2 m; apparent width around 20 m, Table 1) with a wedge-

shaped geometry (Figs. 6, 8A). The complex occupies a very small area (only 1%) in the bedform section, in which only 7 set bodies were identified. The set bodies show a higher proportion of clasts of opaque heavy minerals in comparison to the other complexes in the study section (Fig. 8C). Regarding aeolian stratification types, the set bodies that comprise the first complex are usually composed of wind-ripple/grainflow couplets (interbedding between wind-ripple lamination-dominated and grainflow-dominated intervals). Palaeocurrent distribution is bimodal, spanning from a 60° to 125° mode to a 320° to 360° mode (Fig. 9). From the few preserved bounding surfaces, two measurements of dip-azimuth were obtained, 120° and 349°. In particular, the oldest set body preserved within this complex is different in some aspects from the rest of the sets of the studied section (Fig. 8A). Texturally, the sandstones that comprise the first set are moderately sorted, having a higher proportion of very fine- and coarse-grained sand in comparison to other set bodies. The dominant stratification types in the first set body are wind-ripple lamination and grainfall lamination, and grainflow strata are lacking. Also, a stratum of adhesion ripples (Fig. 8B) is found in this set, the only clear sign of humidity observed in the study section. The dip angle of the cross-stratification in the first set is around 10° towards 340°. Even if this complex was eroded to a great extent before the deposition of the subsequent complex, the characteristics of the preserved set bodies show evidence of particular accumulation conditions, different from the following complexes.

*Interpretation.* A bimodal distribution of palaeocurrent directions and bounding surface's dip-azimuths, coupled with individual cross-stratification in set bodies dipping oblique to the strike of it associated lower bounding surface and to the largest axis of the set body, is consistent with the architecture expected for a sinuous linear dune with a sustained longitudinal dynamic (dominant elongation, minor lateral migration; Tsoar, 1982; Figs. 55

and 77 of Rubin, 1987; Rubin *et al.*, 2008). In this case, each opposing side of the same dune crest is responsible for the formation of set bodies with one of the two palaeocurrent modes. The strike of the bounding surfaces and the orientation of the set body's largest axis is sub-parallel to the dunes elongation direction. On the other hand, the texture and stratification types of the oldest preserved set body indicate that its associated original bedform lacked an active slipface and could represent the remains of an incipient bedform like a dome dune (*Sensu* Pye and Tsoar, 2009; Warren, 2013).

The spatial relationship between the first set body and the rest of the sets in this complex is similar to which it could be expected from a growing, elongating sinuous linear dune, as shown in the models of Bristow *et al.* (2000; their stage 1, Fig. 3), Rubin *et al.* (2008) and in the models built for this study (next section) which emulate the behaviour and growth of *seif* dunes. Taking those models into consideration, the first set of the complex is likely the remains of a linear dune tip or nose, later covered by the deposits of the same elongating dune. In this way, the sedimentary architecture of Complex 1 can be explained by the growth (i.e. size increment) and longitudinal behaviour (i.e. sustained longitudinal dynamics) of a single, simple linear dune or *seif*.

*Complex 2*

*Description.* Complex 2 is characterized by the occurrence of very large-scale set bodies (maximum thickness average at 4-5 m, and up to 8.5 m; apparent width average at 65-66 m, Table 1, Figs. 6, 8) occupying a large area (around 47%) of the study section. Set bodies in this complex show a clear bimodal palaeocurrent and bounding surface dip-azimuth distribution, dependent on the position in the section. A 315° to 15° palaeocurrent mode is dominant in the northern flank of the preserved bedform section, while a 45° to 165° mode is

dominant in the southern flank (Fig. 9, considering both wedge and trough-shaped set bodies). Bounding surfaces in the flank sectors are planar/tangential in shape and have dip-azimuths from 315° to 0° in the northern flank and from 100 to 150° in the southern flank. In contrast, bounding surfaces in the crest sector are concave upward and have a bimodal dip-azimuth distribution. Furthermore, large-scale set bodies can also be separated into trough-shaped and wedge-shaped bodies (Table 3, Figs. 6, 8, 9). Trough-shaped bodies (Figs. 8D, 9) are located within the centre of the section, they have a high intra-set body variability of cross-stratification dip-azimuth (low S value, Table 3), and have an acute bimodal palaeocurrent distribution. Wedge-shaped bodies (Figs. 8F, 9) are found in the flank areas; they have fairly constant intra-set cross-stratification dip-azimuth (high S value, Table 3) and show an obtuse bimodal palaeocurrent distribution. Trough-shaped bodies are dominated by wind-ripple/grainflow couplets (Fig. 8E), whereas wedge-shaped bodies are more abundant in wind-ripple lamination, increasing gradually in importance towards the base of the set and away from the section crest until becoming wind-ripple dominated (Fig. 8G). Towards the top of this complex, very small-scale set bodies (maximum thickness average less than 1 m; apparent width average around 12 m) are found in groups between the large-scale sets, bounded within a trough-shaped lower bounding surface (Figs 6, 8D). They comprise a particular population (Tables 1, 2, Fig. 7), despite having little volumetric importance (2% of Complex 2 section).

*Interpretation*. Very much alike Complex 1, the second complex's large trough-shaped bodies found at the bedform centre, characterized by a bimodal palaeocurrent distribution and separated by bounding surfaces stacked in a zigzagging pattern, are consistent with the architecture expected for a sinuous, simple linear dune with a strong longitudinal behaviour (Tsoar, 1982, 1983; Rubin and Hunter, 1985; Rubin, 1987; profiles 4 and 5 of Bristow *et al.*

2000; Rubin *et al.*, 2008). However, the dimensions of the set bodies indicate the presence of a larger bedform in comparison to the first complex. Regarding the wedge-shaped bodies, their palaeocurrent directions, their intra-set body cross-stratification dip-azimuth variability, and the evidence of dominant wind-ripple activity, indicate that they represent relatively stable dune sectors where bedform sinuosity is reduced. Sectors with these characteristics are very common in large linear dunes (larger than *seifs*, with a width over 100 m), where they represent the majority of the bedform section down to the dune toes (Lancaster, 1995), and are herein referred to as dune flanks. The trough-shaped sets on the other hand, are interpreted as the deposits of the more active and sinuous crest area, given their position in the section core, the aeolian stratification types present, the palaeocurrent directions and the intra-set body cross-stratification dip-azimuth variability. Considering that the dip-azimuths of bounding surfaces within this complex are oblique to the palaeocurrent directions of the set bodies they bound, and that such orientation depends on which flank the surfaces are located, they are interpreted as a product of along-crest migration of bedform sinuosity, either in the dune crest or flank sectors (Rubin, 1987; Rubin *et al.*, 2008). The small-scale sets at the top of the complex most likely represent the record of minor, superimposed dunes, developed over the large linear dune mentioned earlier. These sets are only preserved within concave-upward surfaces, which suggest that superimposed bedforms were related to overall erosive sectors of their host bedform and had little potential to be incorporated into the bedform record.

Following this conceptual model, the architecture of Complex 2 is likely the result of a single, large linear dune evolving into a slipfaced linear megadune as superimposed dunes developed (similar to the model presented by Bristow *et al.,* 2000 from modern dunes), while sustaining a dominant longitudinal behaviour.

*Complex 3*

*Description.* Complex 3 is characterized by stacked, intermediate-scale, trough-shaped sets (maximum thickness between 1 and 5 m, mode of 2-3 m; apparent thickness between 5 and 40 m, mode of 23 m, Table 2), better preserved in the southern flank (due to modern erosion of the outcrop, Fig. 6), that occupies a large area in the study section (52%). Soft-sediment deformation related to the subsequent transgression (Strömbäck *et al.*, 2005) has locally modified the upper portions of this complex, but not enough to prevent interpretations (Fig. 6). The palaeocurrents from trough-shaped bodies of this complex show an acute bimodal distribution similar to the trough-shaped bodies of Complex 2 (Fig. 9). They are also characterized by wind-ripple lamination/grainflow couplets that pass abruptly into thin (one or two dm thick) wind-ripple abundant or dominated set body bases (Fig. 4B). Bounding surfaces within this complex are of concave-upwards shape, given the trough shape of the sets they bound, and show a wide dip-azimuth distribution. These dip-azimuths span from 315° to 60° in the northern flank and 50° to 120° in the southern flank (Fig. 9), which can also be inferred from the apparent dip in the architectural panels (Fig. 6). The general dip-azimuth trend is therefore dependent upon position within the section and therefore broadly similar to the bounding surface dip-azimuth trend of Complex 2. The upper surface that separates this complex from overlying marine sandstone and evaporite facies, has been mapped in previous studies (Argüello Scotti and Veiga, 2015). Small-scale, elongated features were apparent in the southern flank of the large-scale preserved bedform both from the surface reconstructions and from direct observation of the outcrops. These are oriented subparallel to the large-scale bedform and have a relief reaching up to 6 metres.

*Interpretation*. The trough-shaped bodies of intermediate scale represent, by their size and position within the section, the migration of superimposed dunes over the large-scale bedform. Therefore, the bounding surfaces within this complex are interpreted as superimposition surfaces. The large-scale bedform associated with this complex lacked an active slipface and its behaviour was controlled by the development of its superimposed dunes (compare to stage 5 of Bristow *et al.,* 2000; GPR profiles of Bristow *et al*., 2007). By similarity in palaeocurrent directions to the trough-shaped sets of the previous complex, it is inferred that the superimposed dune types at megadune crest and upper flanks positions were of linear type and longitudinal behaviour. This is also indicated by the small-scale elongated features observed at the top of the complex, which represent the exceptional preservation of superimposed bedforms oriented subparallel to the large-scale preserved bedform. Other bedforms types, however, could have been present closer to the megadune plinth. Some small-scale features with different orientation and morphometry (asymmetrical section, 2 m relief and 100 m wavelength) are present in the interdune sector and clearly represent other bedform types (Argüello Scotti and Veiga, 2015).

Considering the characteristics of Complex 3, its deposition can be associated to the development of a slipfaceless linear megadune, likely of compound type (McKee, 1979). The overall dip-azimuth distribution of the bounding surfaces, dependent upon position, indicates that superimposition of bedforms was preserved in both flanks of the host bedform. This indicates once again that the major bedform had an overall dominant longitudinal behaviour.

## Perspectives gained from deterministic models

To gain further understanding of the bedform development conditions that could have led to the deposition of each complex, the program BEDFORMS (Rubin, 1987) was used. This software simulates bedforms by 3D surfaces from sine curves, and determines the

sedimentary architecture resulting from the successive positions of such surfaces in time. Given that existing BEDFORMS models for linear dunes (both simple and complex/compound) assume a rise of the accumulation surface (*sensu* Kocurek, 1999) over time (Rubin, 1987; Clemmensen and Tirsgaard, 1990; Bose *et al*., 1999; Scherer, 2000), modelling was aimed at reproducing the sedimentary architecture expected for a simple linear dune under non-accumulation conditions (*sensu* Kocurek, 1999) and compared to the outcrops. Original models available were modified to test two different scenarios for simple, sinuous linear dunes (Fig. 10). Firstly, on Model 1, the effect of bedform growth on sedimentary architecture was tested. The represented bedform has an along-crest sinuosity migration and a lateral component in bedform motion, the latter being an order of magnitude smaller than the former (considering rates observed in modern examples by Tsoar *et al.*, 2004; Bristow *et al.*, 2005; Rubin *et al.*, 2008). Model 2 intends to represent the morphodynamics and resulting sedimentary architecture of a *seif* dune in detail. For that purpose, some of the most remarkable studies on the morphology (Tsoar, 1982; Bullard *et al.*, 1995; Lancaster, 1995; Pye and Tsoar, 2009) and dynamics (Tsoar, 1983, 1986; Livingstone and Thomas, 1993; Livingstone, 2003; Tsoar *et al.*, 2004; Rubin *et al.*, 2008) of small sinuous linear dunes or *seifs* were consulted. The bedform represented has peaks and saddles with a spacing half to that of the wavelength of bedform sinuosity, and a high frequency cyclic variation in the symmetry of the dune section. As in the first model, a lateral migration component in dune migration was added. Lastly, both models have a climbing angle of 0°, to emulate non-accumulation conditions observed in the Troncoso Inferior Member at the study area.

The results from first bedform model show that with an important rate of bedform growth, sinuosity migration of a single dune can result in the deposition of a considerable number of cross-stratified set bodies. This is also apparent from the models developed by Bristow *et al.*

(2000) and Rubin *et al.* (2008). Once the width of the bedform exceeds the sinuosity's amplitude, both flanks of the bedform are incorporated into its record. Moreover, Model 1 shows that as long as the width increment (growth) exceeds the rate of lateral migration, more set bodies will be incorporated into the record of both flanks of the dune with time (Fig. 10). These results are key to explain the sedimentary architecture observed in the study section, especially for Complexes 1 and 2, highlighting that a single dune can give origin to a high number of set bodies separated by sinuosity migration surfaces that generate a zigzagging arrangement of bounding surfaces at the section centre (see crest sector, indicated in Fig. 6A, occupying the center of the panel in Fig 6B. Closeup in Fig 8A).

The results from the second model show the expected effect of peaks and saddles on the angle formed between the bedform orientation and the two modes in cross-stratification dip directions observed in the set bodies (Fig. 10). While the peaks are in the southern bends, or meanders, of the dune, the saddles are in the northern counterparts. As a result, the depositional areas corresponding to southern flanks (downdrift of a peak) are dipping in a direction closer to parallel to the main bedform orientation, when compared to depositional areas on the northern flanks. This is evident by the strike of the cross-stratification in Model 2, and in classical field models (Fig. 13 of Tsoar, 1982; Fig. 9 of Tsoar, 1983). More information on the actual cross-stratification dip directions of modern dunes would be necessary to confirm such palaeocurrent distribution. So far, the results of Model 2, based on field evidence (Tsoar, 1982, 1983; Bullard *et al*., 1995; Lancaster, 1995; Pye and Tsoar, 2009), can explain the relationship between overall bimodal palaeocurrent pattern and bedform orientation registered in the Troncoso Aeolian System record.

## Relative chronology of cross-stratified set bodies

To analyse the internal relative chronology of set bodies within architectural complexes, a relative superposition order was built from the architectural panels (in a similar approach as Bristow *et al.*, 2005; their Fig. 4). Because the complexity of the stacking, at an early stage the chronology is divided, and each flank of the study section (north flank and south flank) has an independent chronology. As a result, each set body is identified by a letter ("c" for centre, indicating the initial chronology, "n" for northern flank and "s" for southern flank) and a number (Fig. 6).

The resulting chronostratigraphic scheme (Fig. 11) confirms that the oldest sedimentary bodies lie at the section core and indicates the general trend, already suggested by the complexes' architecture and further confirmed by their distribution, that the record of the studied bedform was deposited from a core outward, forming what can be described as a concentric record. From Complex 1 into Complex 2, there is a noticeable asymmetry in this concentric distribution, being the northern flank the one with the most perceivable expansion in relation to the position of the dune core. On Complex 3 however, this asymmetry is reverted, being the southern flank the one that experienced the biggest expansion from the previous complex. The asymmetry in both complexes cannot be precisely quantified because of the discontinuous record in the northern flank.

## Distribution of architectural complexes

The distribution of each architectural complex was analysed across a width-corrected study section, in order to better represent the actual dimensions in a transverse cut of the megadune. Over this corrected section, the general distribution of the complexes was mapped from the sedimentary logs and from virtual logs in the architectural panel (Fig. 12), which allowed for

determining areal percentage occupied by each complex, measuring their width and height, contrasting the abundance in each sector, and establishing superposition relationships between the complexes.

Complex 2 and 3 comprise almost the whole megadune record, combining for 99% of the section area. These complexes share the record in similar parts (Fig. 12). While Complex 2 is more abundant in the section centre, Complex 3 is far more abundant towards the megadune flanks. Each complex extends successively higher in the body of the preserved bedform and occupies a wider lateral section than the previous complex. Complex 1 has a corrected width of 50 m and around 2 m in height, Complex 2 has a corrected width of around 350 m and a height of approximately 20 m, and Complex 3 has a corrected width of 860 m with a preserved height of 24 m. As such, the distribution of the complexes could be described as concentric, and it is yet another evidence of the bedform record being constructed from a core outward.

At this point it is important to consider the distribution of marine reworking facies that overlie the study section, studied by Strömbäck *et al.* (2005) and mapped by Argüello Scotti and Veiga (2015). These facies are believed to have been formed by saturation and wave action during marine flooding, leading to collapse and remobilization of dune sand. They are nearly absent in the dune crest but are thickest in dune flanks and interdune sectors. Therefore, it is interpreted that aeolian sand remobilization from the crest to the flank sectors has reduced preserved bedform height and the relative volumetric importance of Complex 3, which accounts for its low proportion in the crest sector.

# DISCUSSION

## Conceptual development model of the studied megadune

Data analysis from this study demonstrates that each complex has been formed by a particular phase in bedform development, in which a combination of a specific bedform behaviour, growth, and evolution resulted in a particular sedimentary architecture style. In this regard, we consider the terms "evolution", "behaviour" and "growth" to refer to the long-term changes in shape, dynamics and scale of a bedform, respectively, while bedform "development" is considered as the sum of the long-term changes over those variables. Each phase of bedform development can be related to different bedform configurations. Overall, the deposits of the studied preserved bedform record a story of gradual development though the configurations of a small *seif* dune (likely also from an incipient bedform), a large linear dune, a slipfaced linear megadune and finally a slipfaceless linear megadune (Fig. 13).

Analysis of Complex 1, indicates that the oldest registered phase of bedform development was characterized by the development of a small *seif* dune from an incipient bedform, possibly a dome dune or the tip of a *seif* dune, within a deflationary context associated with the development of a sand drift surface (Fig. 13A).

Complex 2 represents the second phase in bedform development (Fig. 13B), likely triggered by the continuation of the drying-upwards trend and the increase in sand availability. The initiation of this phase is related to the evolution of a large linear dune from the previous small *seif*. This large linear dune had well-developed flanks and plinths and a more sinuous and mobile crest. Gradual growth of this bedform eventually allowed for superimposed dunes to develop on its flanks, evolving as a result into a slipfaced linear megadune. The change in the overall sedimentary architecture produced by this evolution was minimal as superimposed set bodies make only 2% of the complex section area.

Complex 3 represents the third and final phase in bedform development, related to a slipfaceless linear megadune configuration (Fig. 13C). This evolution results in a sedimentary architecture characterized by medium-scale set bodies, bounded by superimposition surfaces. Therefore, evolution to a slipfaceless megadune (start of Phase 3) seems to provoke a relevant impact in the style of sedimentary architecture, in contrast to the initial change in dune configuration form large dune to a slipfaced megadune (Phase 2).

The start and subsequent intensification of aeolian dune construction is most likely the continuation of a drying-upwards trend registered through the Lower Troncoso Member (Veiga *et al.*, 2005). The oldest preserved deposits in Complex 1 still show some signs of deposition upon a damp accumulation surface, and, as drier conditions prevailed, gradually more sand might have become available triggering previously protracted aeolian dune construction. Therefore, sand availability might be the conditioning factor behind bedform evolution into large-size configurations. However, the full range of controls that caused the system to undergo considerable pattern coarsening, and transition from small dunes into megadunes, is speculative from the available data and not considered in this study.

The inferred development of the studied megadune is similar in many ways to the model of bedform development presented by Bristow *et al.* (2000), built from several GPR transects in along the tip of a large, sinuous linear megadune in Namibia. The aforementioned dune has a sedimentary architecture similar to that of Complexes 1 and 2 in the Troncoso record. Furthermore, it changes laterally though bedform configurations similar to the ones inferred to have deposited the complexes described in the present study. However, the sedimentary architecture of the Troncoso record related to the simple dune configuration is more complex, formed by a larger number of cross-stratified set bodies. This difference is most likely related to a longer-lived linear dune configuration in the Troncoso example, along with consistent gradual bedform growth and a dominant longitudinal behaviour.

## Conditioning factors over the development of the studied bedform

The internal characteristics of the architectural complexes and their distribution (Figs. 6, 9, 11, 12) indicate that the preserved bedform had an overall consistent and dominant longitudinal behaviour throughout its recorded development. This does not prove that the bedform did not undergo lateral migration; in fact, the construction and distribution of each complex has a certain degree of asymmetry that indicates a lateral component in migration (Figs. 6, 12). However, through all three complexes, evidence indicates that the bedform produced deposition on both flanks, even under the effect of lateral migration. Considering that this bedform never produced accumulation (*sensu* Kocurek, 1999), then the process that allows both flanks to be preserved must be bedform growth (i.e. increment in bedform scale) and not accretion (i.e. rise in the accumulation surface). Therefore, during the development of the studied bedform, lateral migration rates were surpassed by a growth component. Even if growth in one flank was favoured in relation to the other, both flanks showed an overall long-term growth. From all of the above, bedform growth together with a dominant longitudinal behaviour were the crucial factors in shaping the sedimentary architecture of the preserved bedform.

It is likely that after the bedform had stopped its growth as a megadune, a little component of lateral migration could have completely changed its sedimentary architecture given sufficient time. However, such lateral migration rate should have been consistent and sustained through the extended periods of time that these bedforms need to reach equilibrium with environmental conditions (which are rarely achieved). In this case, marine flooding of the Troncoso Sand Sea hindered further development of this bedform.

Since the genetic link between different types of linear aeolian bedforms has been mostly inferred, and rarely documented (Warren, 2013), the record of the studied preserved megadune provides an exceptional example of the evolution between different types of

aeolian linear bedforms during the development of a large linear megadune. It documents the link between small *seif* dunes, large linear dunes and linear megadunes, and in particular, the scale at which the transition between a simple dune and a megadune occurs, that is as the bedform width reaches 300-400 m. The particular growth-dominated development of the studied bedform seems to be the main reason behind the preservation of bedform evolution.

**Sinuosity migration surfaces: a bounding surface type for simple linear dunes**

Detailed analysis of the architecture of Complexes 1 and 2, together with the lessons learned from deterministic models and previous studies of linear dune architecture and behaviour (Tsoar, 1983; Rubin, 1987; Bristow *et al.*, 2000; Rubin *et al.*, 2008), highlight that the internal architecture of simple sinuous linear dunes can be characterized by the predominance of large-scale bounding surfaces generated by the longitudinal (along-crest) migration of the bedform sinuosity. The term "*sinuosity migration surfaces"* is suggested in this study to refer to such bounding surface type.

The particular characteristics of this bounding surface type are dip-azimuths which are oblique to the palaeocurrent directions of the set bodies they bound and strikes subparallel to the bedform orientation (Fig. 10). If both flanks of the bedform are preserved in the rock record, then two modes of surface dip-azimuths will be recorded. The angle between these two modes will likely be a high obtuse angle and each dip-azimuth mode will be dominant in the respective flank of the bedform record. If, on the other hand, only one flank of the dune is preserved due to a predominance of lateral migration, the dip-azimuth distribution of the preserved surfaces will have only one clear mode. In the context of autocyclic surfaces generated by aeolian bedforms, the hierarchy of sinuosity migration surfaces is lower than that of interdune migration and superimposition surfaces, and higher to that of reactivation surfaces. This surface type introduces a remarkable complexity into the deposits of a simple

dune, and its impact upon identification and sedimentary heterogeneity characterization in this type of deposits must be highlighted.

Estimating bedform orientation from the strike of this bounding surface, although a much more accurate indicator than palaeocurrent orientation, must be exercised with caution. As the two modes of dip-azimuths are not bipolar, one must choose between one of the modes, or perform the bisector between the two. In this regard, more theoretical and field work is needed to determine the causes that lead to a non-bipolar bounding surfaces dip-azimuth distribution.

**Factors conditioning the sedimentary architecture of linear bedforms**

As with any other bedform type, behaviour, growth, and evolution are major factors that condition the resulting sedimentary architecture of aeolian linear bedforms (alongside for example, the relative motion of the accumulation surface). However, some of the discussed factors gain or lose relative importance for this particular bedform type.

What this case study in particular suggests, is that bedform growth can be an important conditioning factor in the long-term development linear bedforms and particularly critical in shaping its internal sedimentary architecture. Growth exponentially reduces the lateral migration rate of a linear bedform by reducing its surface/volume relationship. Furthermore, as growth doesn't potentially impact along-crest sand transport, it should favour a longitudinal bedform behaviour. In other words, growth has a considerable impact in behaviour (i.e. long-term dynamics). This likely indicates that as linear bedforms reach large dune and especially megadune-scale sizes, lateral migration rates can become so low that its influence over the preserved internal architecture could be greatly overshadowed by other factors. The far more mobile transverse ridges (*sensu* Rubin and Hunter, 1985) provide an opposite extreme in relative importance of conditioning factors. In transverse bedforms, any

effect of a growth component will not produce a lasting impact in the sedimentary architecture, due to the far larger migration rates of these bedforms. The overall sedimentary architecture in that case will be more influenced by bedform scale and behaviour along with relative motion of the accumulation surface.

Finally, it must also be considered that the parameters associated to bedform development are ultimately controlled by the larger dunefield self-organization, which dictates the bedform pattern of the system (Kocurek and Ewing, 2005). This can explain why the record of adjacent linear bedforms (or even the record of the same bedform along its extension) can be quite different, as seen in the many dunes studied in the northern extreme of the Namib Sand Sea (Bristow *et al.*, 2000, 2005, 2007).

## Models of linear bedform sedimentary architecture

Considering previous case studies and the example provided in this study, assigning a simple model of the expected sedimentary architecture for sandy, aeolian linear bedforms is far from a simple task. The overall internal architecture of aeolian linear bedforms however, can be considered to vary from two opposite extremes (Fig. 14): a concentric style, where the oldest deposits are found in the bedform core (e.g. bedform studied in this paper), and an asymmetric style, where the oldest deposits are found in one of the flank's extremes (e.g. Station Dune; Bristow *et al.*, 2005). This differentiation can be made for the deposits of both simple and compound/complex bedforms. Bounding surface's dip-azimuths would be bimodal and dependent upon their position in the concentric style, while they would be unimodal and evenly distributed in the asymmetric counterpart. In the concentric style, the architecture will likely be conditioned by growth and/or accretion, along with a strong sustained longitudinal behaviour. If the style of architecture is on the other hand asymmetric, the architecture is likely to have been strongly conditioned by a sustained and consistent

lateral migration. This scheme departs from earlier classifications (Fig. 1) by using a descriptive terminology, independent from the possible mechanisms that may have shaped the sedimentary architecture and from the simple/compound/complex nature of the originating bedform.

Previous studies that have encountered a sedimentary architecture resembling a concentric style, have attributed it to accretion of the bedform pattern (Rubin and Hunter, 1985; Bose *et al.*, 1999). However, Rubin and Hunter (1985) made it clear that the natural conditions necessary for accretion of a bedform pattern of linear dunes that would allow preservation of both flanks in the geological record (with a climbing angle of at least 30°), are very specific and would be extremely uncommon and restricted spatially. Therefore, considering the slow migration rates for these bedforms, sustained bedform growth can be a development scenario far more likely than accretion to account for the preservation of this style of sedimentary architecture. If the notion, under aeolian sequence stratigraphic conceptual framework (Kocurek, 1999), that accumulation is not necessary for preservation is also considered (a common scenario for ancient deposits of linear bedforms; e.g. Entrada Sandstone, Lower Permian Yellow Sands, Botucatu Formation, Troncoso Inferior Member), then the conditions necessary for a linear dune to preserve a more "classic" sedimentary architecture style of bimodal cross-stratification and bounding surface dip directions may not be unusual in cases of preserved bedform topography.

## CONCLUSIONS

The methodology followed in this paper was successful in identifying significant qualitative and quantitative differences within the sedimentary architecture exposed in a natural section of a preserved linear bedform belonging to the ancient Troncoso Sand Sea. These differences allowed for the identification of three different sedimentary architecture styles or

architectural complexes. These were demonstrated to be formed by genetically related, cross-stratified set bodies and bounding surfaces, associated to a specific phase in bedform development in which bedform evolution, behaviour and growth resulted in a relatively homogeneous style of sedimentary architecture.

A conceptual model for the development of the studied preserved bedform was presented, composed by three phases. Phase one comprises a possible incipient bedform (dome dune or *seif* dune tip) evolving into a small linear *seif*. Phase two represents the development of a large linear dune that evolves into a slipfaced linear megadune. Finally, phase three is characterized by a slipfaceless linear megadune coincident to the final preserved morphology of the bedform.

Development of the studied bedform was characterized by sustained growth and a dominant longitudinal behaviour, which were the key parameters shaping its final internal architecture, while the lateral migration component in bedform behaviour was never a critical factor. Preservation of bedform evolution provided a unique example to document the link between different types of linear bedforms.

Characterization of the preserved bedform's record allowed for discussing which parameters are most critical in shaping the sedimentary architecture of linear bedforms. It suggests that growth can be an important factor for this bedform type given their low migration rates, which become exponentially lower as bedforms increase their size.

Finally, linear bedform deposits can be characterized by two contrasting styles of sedimentary architecture: a concentric style, and an asymmetric style. In the former, the oldest deposits are found in the bedform core, while on the latter, the oldest deposits are found in one of the flank's extremes. The characteristics of the bounding surfaces in each case were analysed, and the likely controlling factors behind each style of architecture were determined. Since concentric architecture generated by accretion requires conditions regarded

as very unlikely in nature, consistent bedform growth and dominant longitudinal behaviour can be considered as a likely scenario to account for this architecture type. This possibility indicates that the occurrence of a concentric architecture may not be as unusual in the geological record as previously thought, in cases where linear dunes were associated to exceptional preservation mechanisms.

## ACKNOWLEDGMENTS

This research was funded by the Consejo Nacional de Investigaciones Científicas y Técnicas (CONICET-PIP 112-201101-00322) and through a co-operation agreement between YPF S.A. and the Centro de Investigaciones Geológicas (UNLP-CONICET). The authors are grateful to the insightful comments and suggestions made by Nick Lancaster, Juan Pedro Rodriguez-Lopez, and to two anonymous reviewers. We are also grateful to Nigel P. Mountney, Ernesto Schwarz, Luis A. Spalletti and Bailey A. Lathrop for their encouragement and feedback that though different stages of this study. Nicolás Scivetti and Joaquín Bucher's very valuable assistance in the field are greatly appreciated.

Keywords = Sedimentary architecture, Aeolian linear bedforms, Bedform development, Cretaceous, Neuquén Basin, Troncoso Inferior

## REFERENCES CITED

**Aguirre-Urreta, B., Schmitz, M., Lescano, M., Tunik, M., Rawson, P.F., Concheyro, A., Buhler, M.,** and **Ramos, V.A.** (2017) A high precision U–Pb radioisotopic age for the Agrio Formation, Neuquén Basin, Argentina: Implications for the chronology of the Hauterivian Stage. *Cretaceous Res.*, **75**, 193-204.

**Ahmed Benan, C.A.** and **Kocurek, G.** (2000) Catastrophic flooding of an aeolian dune field: Jurassic Entrada and Todilto formations, Ghost Ranch, New Mexico, USA. *Sedimentology*, **47**, 1069-1080.

**Argüello Scotti, A.** (2017) Origen, arquitectura interna y evolución secuencial del Sistema Eólico Barremiano en el centro-este de la Cuenca Neuquina: modelado tridimensional e implicancias para la caracterización de reservorios de origen eólico (*Doctoral Thesis*). Universidad Nacional de La Plata, La Plata, 235 pp.

**Argüello Scotti, A.** and **Veiga, G.D.** (2015) Morphological Characterization of an Exceptionally Preserved Eolian System: the Cretaceous Troncoso Inferior Member in the Neuquén Basin (Argentina). *Latin Am. J. Sedimentol. Basin Anal.*, **22**, 29-46.

**Bagnold, R.A.** (1941) The Physics of Blown Sand and Desert Dunes. Methuen & Company, London, 265 pp.

**Besly, B., Romain, H.G., Mountney, N.P.** (2018) Reconstruction of linear dunes from ancient aeolian successions using subsurface data: Permian Auk Formation, Central North Sea, UK. *Mar. Petrol. Geol.,* **91**, 1-18.

**Bose, P.K., Chakrabarty, S.** and **Sarkar, S.** (1999) Recognition of ancient eolian longitudinal dunes; a case study in upper Bhander Sandstone, Son Valley, India. *J. Sed. Res.*, **69**, 74-83.

**Bristow, C.S., Bailey, S.D.** and **Lancaster, N.** (2000) The sedimentary structure of linear sand dunes. *Nature*, **406**, 56-59.

**Bristow, C.S., Duller, G.A.T.** and **Lancaster, N.** (2007) Age and dynamics of linear dunes in the Namib Desert. *Geology*, **35**, 555-558.

**Bristow, C.S., Lancaster, N.** and **Duller, G.A.T.** (2005) Combining ground penetrating radar surveys and optical dating to determine dune migration in Namibia. *J. Geol. Soc. London*, **162**, 315-321.

**Bullard, J.E., Thomas, D.S.G., Livingstone, I.** and **Wiggs, G.F.S.** (1995) Analysis of linear sand dune morphological variability, southwestem Kalahari Desert. *Geomorphology*, **11**, 189-203.

**Cignoni, P., Corsini, M.** and **Ranzuglia, G.** (2008) MeshLab: an open-source 3D mesh processing system. *ERCIM News*, **73**, 45-46.

**Clemmensen, L.B.** (1989) Preservation of interdraa and plinth deposits by the lateral migration of large linear draas (Lower Permian Yellow Sands, northeast England). *Sed. Geol.*, **65**, 139-151.

**Clemmensen, L.B.** and **Tirsgaard, H.** (1990) Sand-drift surfaces: a neglected type of bounding surface. *Geology*, **18**, 1142-1145.

**Collinson, J.D., Mountney, N.P.** and **Thompson, D.B.** (2006) Sedimentary Structures. Terra, Harpenden, 292 pp.

**Dajczgewand, D., Nocioni, A., Fantin, M., Minniti, S., Calegari, R.** and **Gavarrino, A.** (2006) Lower Troncoso eolian bodies identification in the Neuquen Basin, Argentina: a different approach and some geological implications. *Extended abstract from the 9th Simposio Bolivariano - Exploración Petrolera en las Cuencas Subandinas*, Cartagena, Colombia.

**Glennie, K.W.** (1972) Permian Rotliegendes of Northwest Europe interpreted in light of modern desert sedimentation studies. *AAPG Bull.*, **56**, 1048-1071.

**Groeber, P.** (1946) Observaciones geológicas a lo largo del meridiano 70. Hoja Chos Malal. *Revista de la Sociedad Geológica Argentina,* **1**, 177-208.

**Havholm, K., Kocurek, G.** (1994) Factors controlling aeolian sequence stratigraphy: clues from super bounding surface features in the Middle Jurassic Page Sandstone. *Sedimentology*, **41**, 913-934.

**Hodgetts, D.** (2009) LiDAR in the environmental sciences: geological applications. In: *Laser*

*Scanning for the Environmental Sciences* (Eds G. Heritage and A. Large), pp. 165-179. Wiley-Blackwell, Oxford.

**Howell, J.A., Schwarz, E., Spalletti, L.A.** and **Veiga, G.D.** (2005) The Neuquén Basin: an overview. In: *The Neuquén Basin, Argentina: A Case Study in Sequence Stratigraphy and Basin Dynamics* (Eds G.D. Veiga, L.A. Spalletti, J.A. Howell and E. Schwarz), *Geol. Soc. London Spec. Publ.*, 252, 1-14.

**Hunter, R.E.** (1977) Basic types of stratification in small eolian dunes. *Sedimentology*, **24**, 361-387.

**Kocurek, G.** (1999) The aeolian rock record (Yes, Virgina, it exists, but it really is rather special to create one). In: *Aeolian Environments Sediments and Landforms* (Eds A.S. Goudie, I. Livingstone and S. Stokes), pp. 239-259. John Wiley and Sons, Chichester.

**Kocurek, G.** and **Dott, R.H.** (1981) Distinctions and Uses of Stratification Types in the Interpretation of Eolian Sand. *J. Sed. Res.*, **51**, 579-595.

**Kocurek, G.** and **Ewing, R.C.** (2005) Aeolian dune field self-organization - Implications for the formation of simple versus complex dune-field patterns. *Geomorphology*, **72**, 94-105.

**Kocurek, G.** and **Havholm, K.G.** (1993) Eolian sequence stratigraphy— a conceptual framework. In: Siciliclastic Sequence Stratigraphy (Eds P. Weimer and H.W. Posamentier), *AAPG Mem.,* 58, 393-409.

**Kocurek, G., Knight, J.** and **Havholm, K.** (1991) Outcrop and semi-regional three-dimensional architecture and reconstruction of a portion of the eolian Page Sandstone (Jurassic). In: *The Three-Dimensional Facies Architecture of Terrigenous Clastic Sedi-Ments and Its Implications for Hydrocarbon Discovery and Recovery* (Eds A.D. Miall and N. Tyler), *SEPM Spec. Publ.*, **3**, 25-43.

**Lancaster, N.** (1995) Geomorphology of Desert Dunes. Routledge, London, 290 pp.

**Lancaster, N.** (1982) Linear dunes. *Prog. Phys. Geogr.*, **6**, 475-504.

**Lazo, D.G.** and **Damborenea, S.E.** (2011) Barremian bivalves from the Huitrín Formation, west-central Argentina: taxonomy and paleoecology of a restricted marine association. *J. Paleontol.*, **85**, 719-743.

**Livingstone, I.** (2003) A twenty-one-year record of surface change on a Namib linear dune. *Earth Surf. Proc. Land.*, **28**, 1025-1031.

**Livingstone, I.** and **Thomas, D.S.G.** (1993) Modes of linear dune activity and their palaeoenvironmental significance: an evaluation with reference to southern African examples. In: *The Dynamics and Environmental Context of Aeolian Sedimentary Systems* (Ed K. Pye), *Geol. Soc. London Spec. Publ.*, 72, 91-101.

**Livingstone, I.** and **Warren, A.** (1996) Aeolian Geomorphology: an Introduction. Longman, Essex, 221 pp.

**McKee, E.D.** (1979) Introduction to a Study of Global Sand Seas. In: *A Study of Global Sand Seas* (Ed E.D. McKee), pp. 3-19. United States Geological Survey, Washington D.C.

**McKee, E.D.** and **Tibbitts, G.C.** (1964) Primary Structures of a Seif Dune and associated deposits in Libya. *J. Sed. Petrol.*, **34**, 5-17.

**Mountney, N.P.** (2006) Eolian Facies Models. In: *Facies Models Revisited* (Eds H.W. Posamentier and R.G. Walker), *SEPM Spec. Publ.*, **84**. 19-83.

**Pye, K.** and **Tsoar, H.** (2009) Aeolian Sand and Sand Dunes. Springer, Berlin, 458 pp.

**Rarity, F., van Lanen, X.M.T., Hodgetts, D., Gawthorpe, R.L., Wilson, P., Fabuel-Perez, I.,** and **Redfern, J.** (2014) LiDAR-based digital outcrops for sedimentological analysis: workflows and techniques. In: Sediment-Body Geometry and Heterogeneity: Analogue Studies for Modelling the Subsurface (Eds A. W. Martinius, J.A. Howell, T.R. Good), *Geol. Soc. London Spec. Publ.*, 387, 153-183.

**Rodríguez-López, J.P., Clemmensen, L.B., Lancaster, N., Mountney, N.P. and Veiga, G.D.** (2014) Archean to Recent aeolian sand systems and their sedimentary record: Current

1 understanding and future prospects. *Sedimentology*, **61**, 1487-1534.

2 **Rodríguez-López, J.P., Meléndez, N., De Boer, P.L., Soria, A.R.** (2008) Aeolian sand sea
3 development along the mid-Cretaceous western Tethyan margin (Spain): Erg sedimentology
4 and palaeoclimate implications. *Sedimentology*, **55**, 1253-1292.

5 **Rodríguez-López, J.P., Meléndez, N., Boer, P.L. De, Soria, A.R., Liesa, C.L.** (2013)
6 Spatial variability of multi-controlled aeolian supersurfaces in central-erg and marine-erg-
7 margin systems. *Aeolian Research*, **11**, 141-154.

8 **Roskin, J., Tsoar, H., Porat, N., Blumberg, D.G.** (2011) Palaeoclimate interpretations of
9 Late Pleistocene vegetated linear dune mobilization episodes: Evidence from the
10 northwestern Negev dunefield, Israel. *Quatern. Sci. Rev.,* **30**, 3364-3380.

11 **Rubin, D.M.** (1987) Cross-Bedding, Bedforms, and Paleocurrents. *Concepts in*
12 *Sedimentology and Paleontology*, **1**, 187 pp.

13 **Rubin, D.M.** and **Hunter, R.E.** (1985) Why deposits of longitudinal dunes are rarely
14 recognized in the geologic record. *Sedimentology*, **32**, 147-157.

15 **Rubin, D.M., Tsoar, H.,** and **Blumberg, D.G.** (2008) A second look at western Sinai seif
16 dunes and their lateral migration. *Geomorphology*, **93**, 335-342.

17 **Scherer, C.M.S.** (2000) Eolian dunes of the Botucatu Formation (Cretaceous) in
18 southernmost Brazil: Morphology and origin. *Sed. Geol.*, **137**, 63-84.

19 **Steele, R.P.** (1983) Longitudinal Draa in The Permian Yellow Sands of North-East England.
20 *Dev. Sedimentol.*, **38**, 543-550.

21 **Strömbäck, A., Howell, J.A.** and **Veiga, G.D.** (2005) The transgression of an erg -
22 sedimentation and reworking/soft-sediment deformation of aeolian facies: the Cretaceous
23 Troncoso Member, Neuquén Basin, Argentina. In: *The Neuquén Basin, Argentina: A Case*
24 *Study in Sequence Stratigraphy and Basin Dynamics* (Eds G.D. Veiga, L.A. Spalletti, J.A.
25 Howell and E. Schwarz), *Geol. Soc. London Spec. Publ.*, 252, 163-183.

**Tsoar, H.** (1982) Internal structure and surface geometry of longitudinal (seif) dunes. *J. Sed. Res.*, **52**, 823-831.

**Tsoar, H.** (1983) Dynamic processes acting on a longitudinal (seif) sand dune. *Sedimentology*, **30**, 567-578.

**Tsoar, H.** (1986) The advance mechanism of Longitudinal Dunes. In: *Physics of Desertification* (f. El-Baz and H. Mohammed) pp. 241-250. Martinus Nijhoff, Dordrecht.

**Tsoar, H.** (1989) Linear dunes - forms and formation. *Prog. Phys. Geogr.*, **13**, 507-528.

**Tsoar, H., Blumberg, D.G.** and **Stoler, Y.** (2004) Elongation and migration of sand dunes. *Geomorphology*, **57**, 293-302.

**Veiga, G.D., Howell, J.A.** and **Strömbäck, A.** (2005) Anatomy of a mixed marine-non-marine lowstand wedge in a ramp setting. The Record of a Barremian-Aptian complex relative sea-level fall in the central Neuquen Basin, Argentina. In: *The Neuquén Basin, Argentina: A Case Study in Sequence Stratigraphy and Basin Dynamics* (Eds G.D. Veiga, L.A. Spalletti, J.A. Howell and E. Schwarz), *Geol. Soc. London Spec. Publ.*, 252, 139-162.

**Warren, A.** (2013) Dunes: Dynamics, Morphology, History. Wiley-Blackwell, Chichester, 236 pp.

**Wilson, I.G.** (1972) Aeolian bedforms-their development and origins. *Sedimentology*, **19**, 173-210.

**Wu, C.** (2011) VisualSFM: A Visual Structure from Motion System. *Retrieved from http://ccwu.me/vsfm/*.

**Figure 1**
Argüello Scotti and Veiga
(full width - 170 mm x 144 mm)

| | | |
|---|---|---|
| THEORETICAL MODELS (Rubin and Hunter, 1985) (Clemmensen 1989) | "ACCRETION" 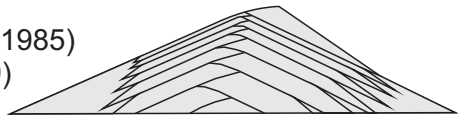 Bagnold (1941) Tsoar (1982) Rubin and Hunter (1985) | "LATERAL MIGRATION" 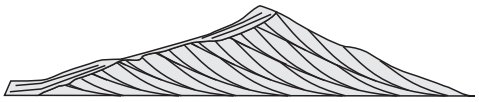 Rubin and Hunter (1985) |
| 3D MODELS/ RESULTANT ARCHITECTURE (Rubin, 1987) | 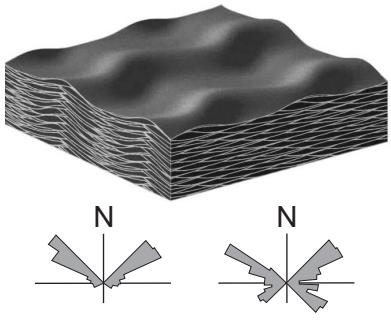  | 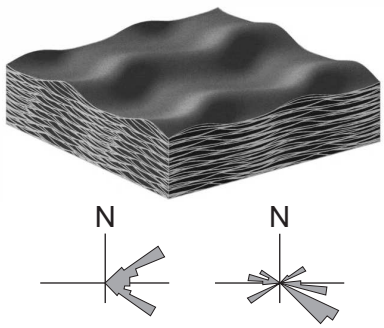  |
| PROCESSES (Tsoar, 2004) | elongation | elongation + lateral migration |
| DYNAMICS | pure longitudinal | longitudinal/oblique |
| ANCIENT EXAMPLES | Bhander Sandstone - Bose *et al.* (1999)<br>L.P.Y.S. - Steele (1983); Clemmensen (1989) | Botucatu Fm. - Scherer (2000)<br>L.P.Y.S. - Clemmensen (1989)<br>Entrada Sst - Ahmed Benan and Kocurek (2000)<br>Escucha Fm. - Rodríguez-López *et al.* (2008) |

**Figure 2**
Argüello Scotti and Veiga
(column width - 80 x 86 mm)

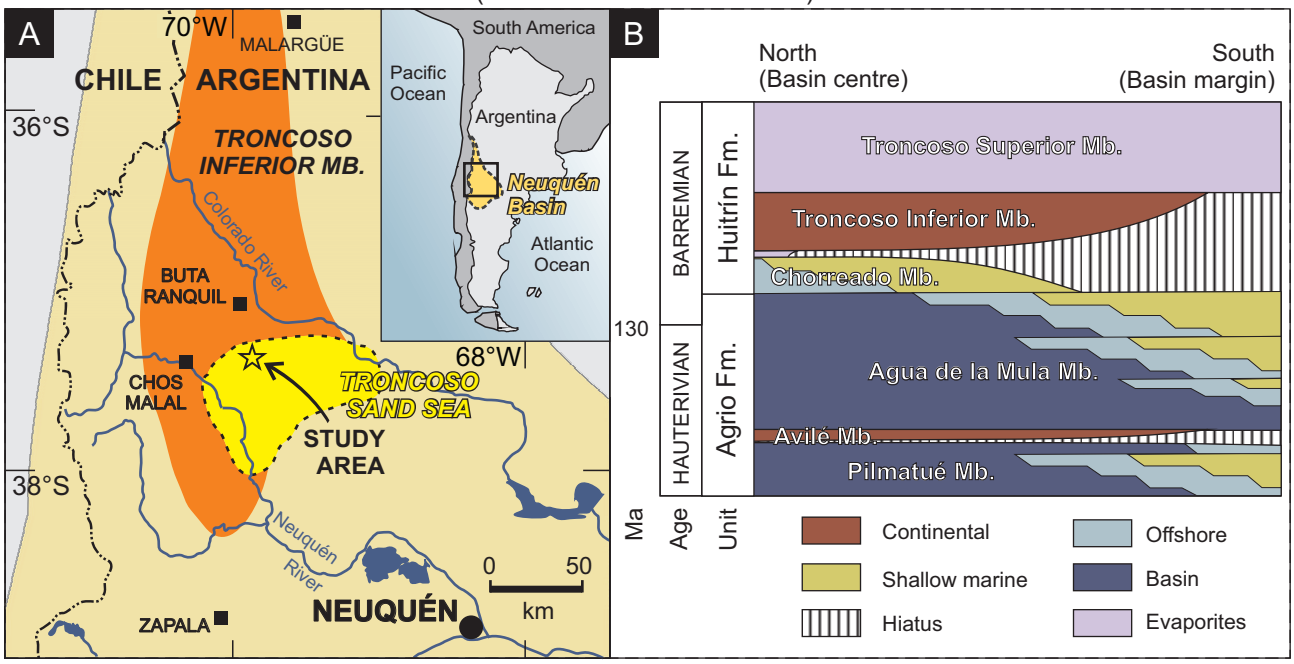

**Figure 3**
Argüello Scotti and Veiga
(full width - 170 mm x 149 mm)

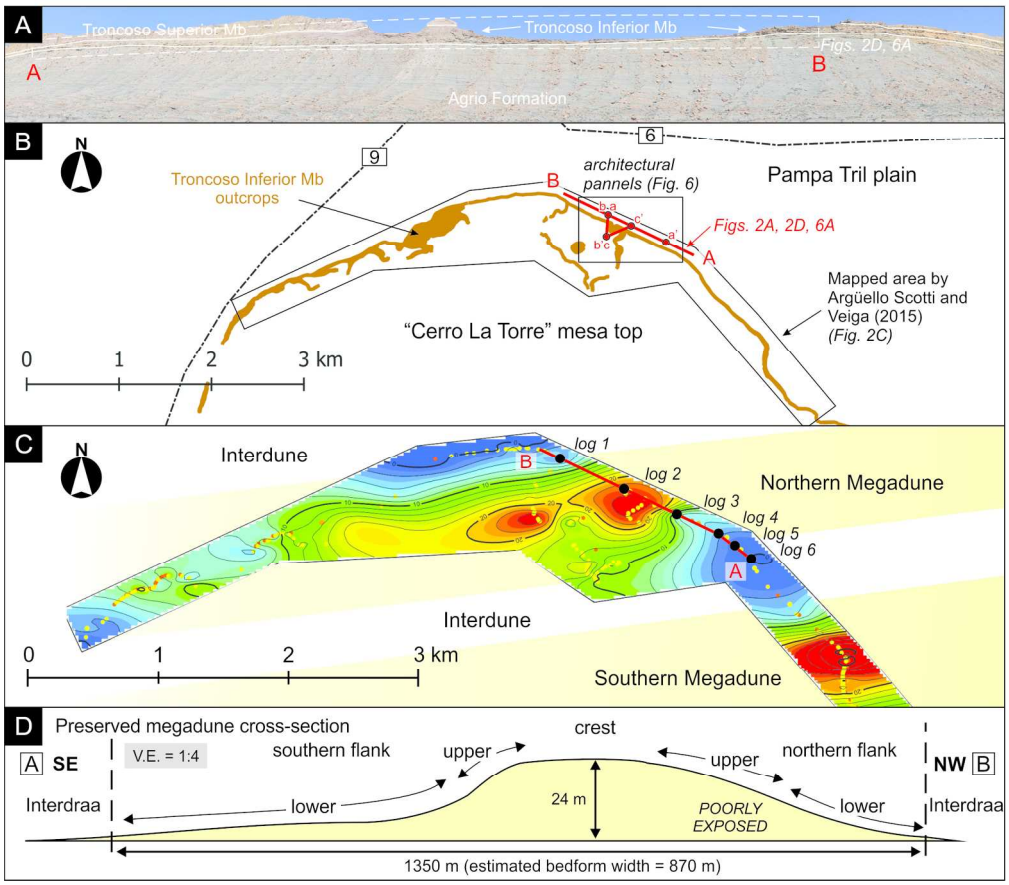


Figure 3. Study area and section, and previous morphology studies in the locality. A) View of the Troncoso Inferior section in the study area, seen from the North. B) Map of the Troncoso Inferior Member outcrops and provincial roads around the study area, showing the location of the study section and the extension mapped in Argüello Scotti and Veiga (2015). C) Thickness map of the study interval in the study area, revealing the location, dimensions and orientation of the large-scale preserved bedforms. D) Study interval's thickness variation in the study section, flattened at the base, showing external geometry features of the preserved bedform, which are further used as reference for the position of internal sedimentary bodies and surfaces.

170x162mm (300 x 300 DPI)

**Figure 4**
Argüello Scotti and Veiga
(full width - 170 mm x 170 mm)

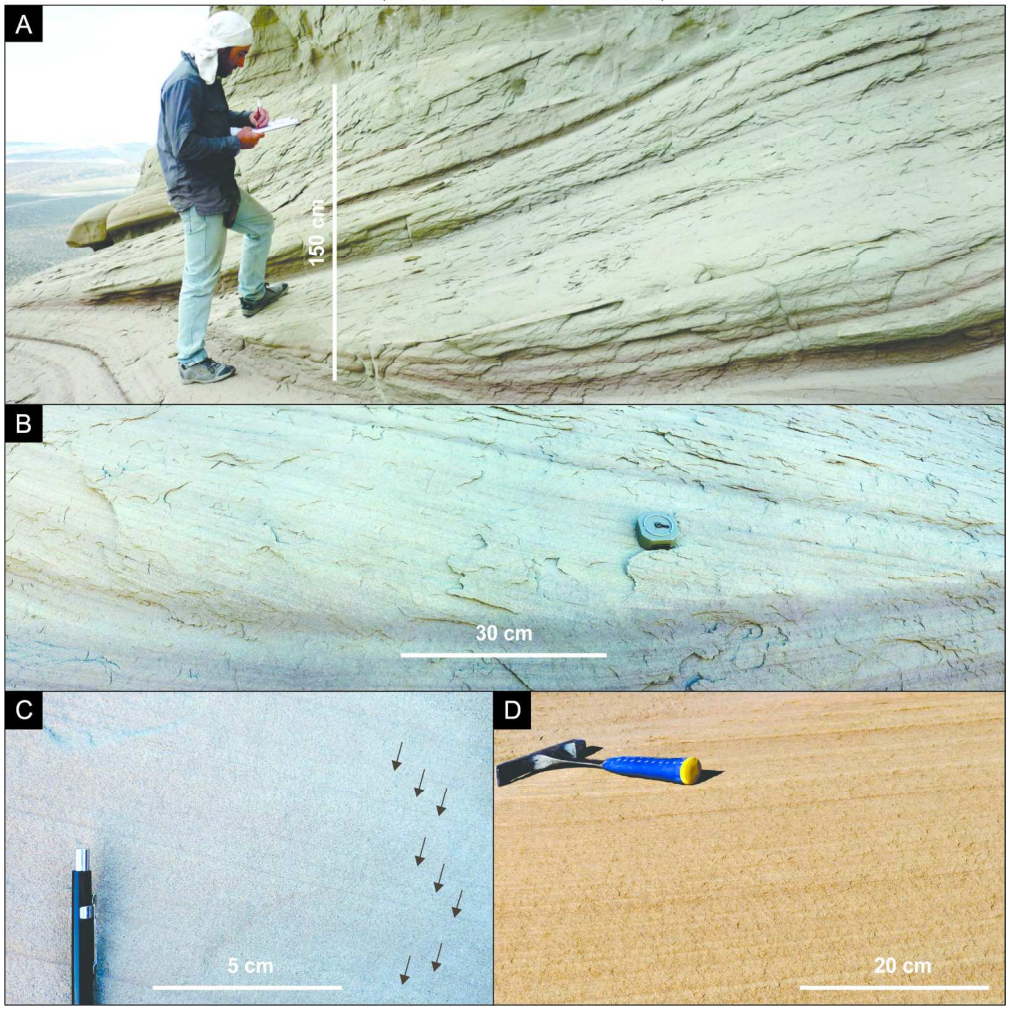


Figure 4. Sedimentary facies and stratification types identified in the study interval. A) Large-scale cross-stratified sandstones passing downwards into subhorizontal laminated sandstones. B) Clearly recognizable individual high-angle grainflow strata wedging out into low-angle wind-ripple lamination (climbing translatent strata) in the bottom of a cross-stratified set body. C) Grainflow strata separated by thin grainfall laminae (marked by black arrows). D) Close up of a wind-ripple lamination dominated sector of a cross-stratified set body.

170x182mm (300 x 300 DPI)

**Figure 5**
Argüello Scotti and Veiga
(2/3 page - 112 mm x 134 mm)

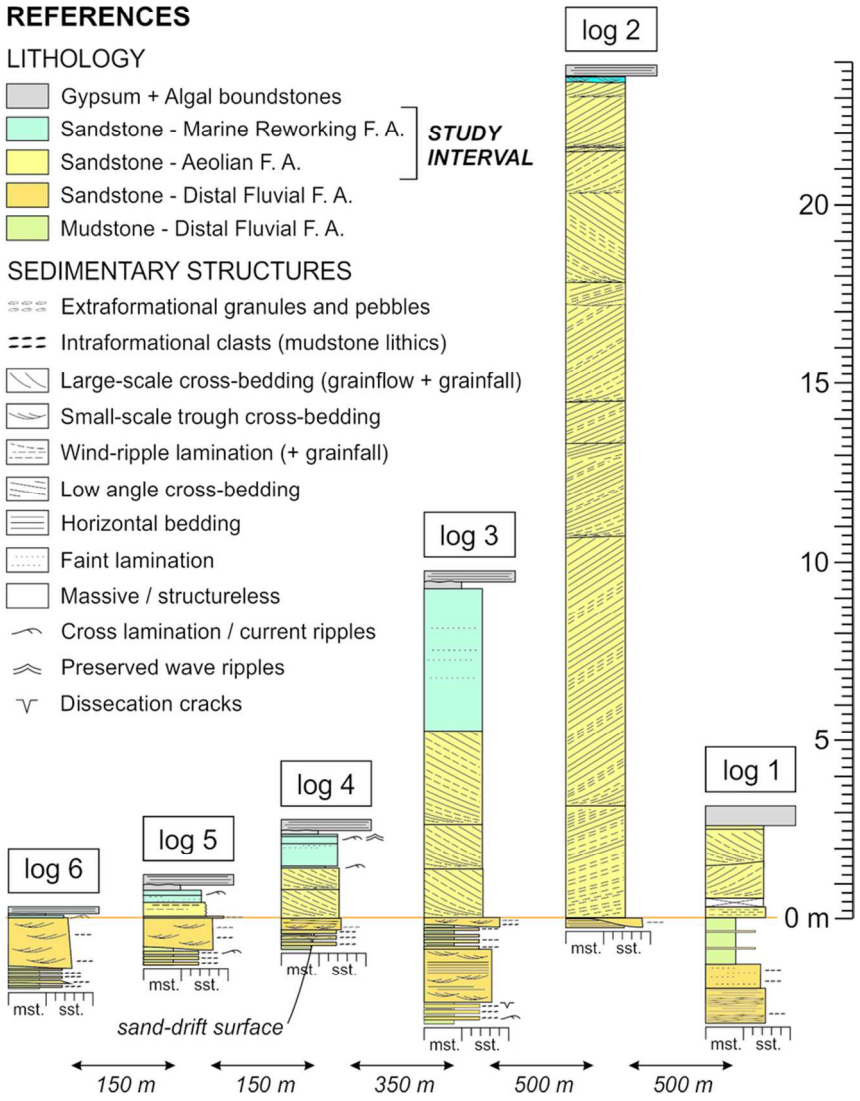


Figure 5. Sedimentary logs measured in the study section (location in Fig. 3), levelled at the base of the Troncoso Erg System record. The base of this record is represented in the study area by a sharp planar surface interpreted by previous studies as a sand-drift surface (see text for discussion). Note how sandstone bodies belonging to the aeolian facies association thin out laterally in the interdune sectors.

78x110mm (300 x 300 DPI)

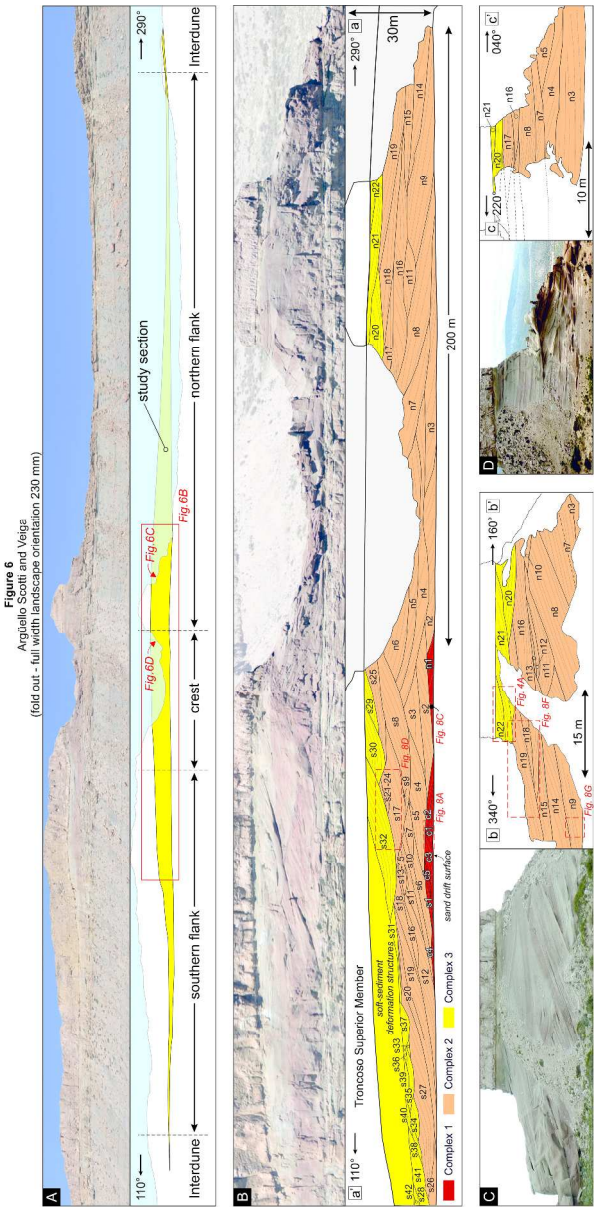


Figure 6. Sedimentary architecture of the studied section. A) Close up of the photomosaic shown in Fig. 2A, with the study section marked in yellow. B) Architectural panel a-a' (location on Figs. 2B, 6A). C) Architectural panel b-b' (Location on Fig. 2B, 6A). D) Architectural panel c-c' (Location on Fig. 2B, 6A). All panels show identified architectural complexes (see text for further details), discerned by colour, and cross-stratified set body identifications tags. Each set body is identified by a letter, "c" for centre, "n" for northern flank and "s" for southern flank, and a number.

360x733mm (300 x 300 DPI)

**Figure 7**
Argüello Scotti and Veiga
(2/3 page or 1 column)

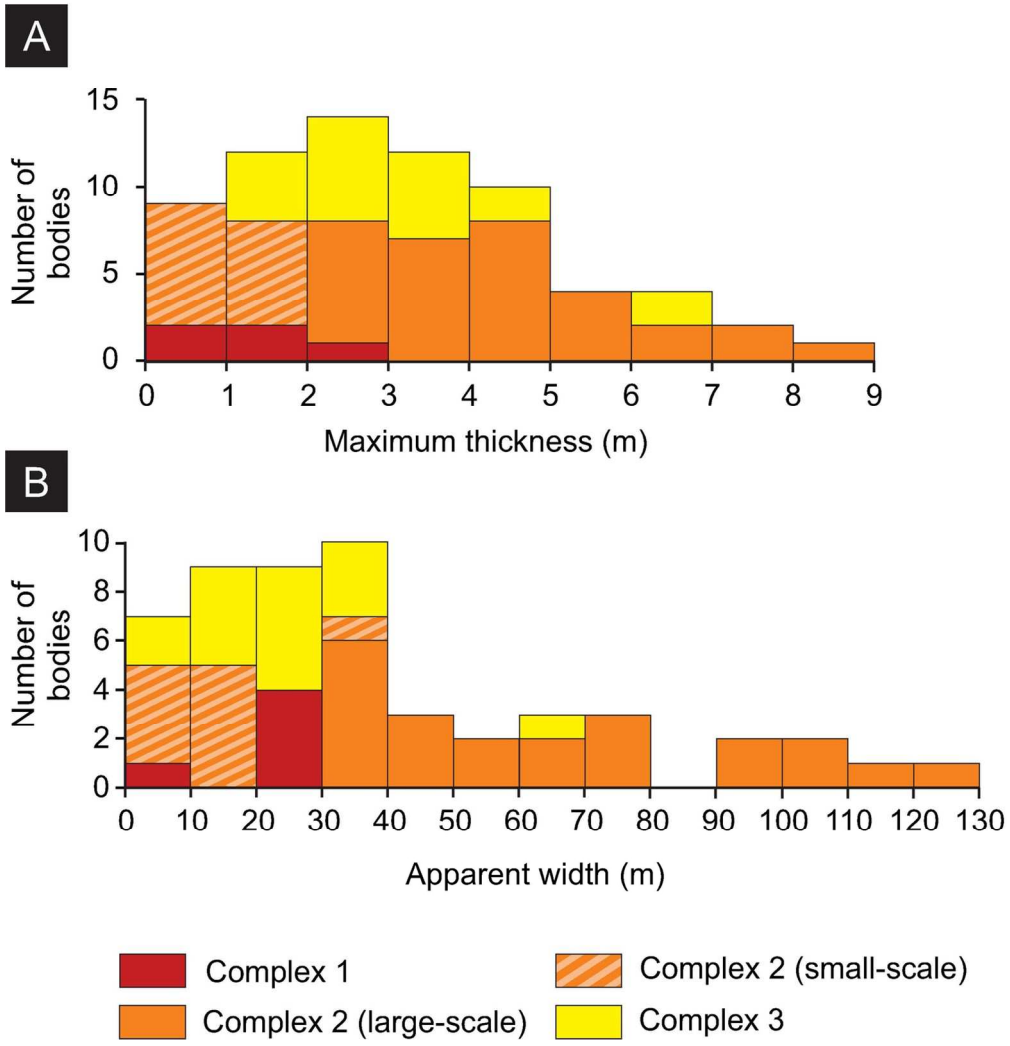


Figure 7. Histograms indicative of cross-stratified set body scale, discriminated by architectural complex. A) Frequency of set body's maximum thickness. B) Frequency of set body's apparent width.

129x150mm (300 x 300 DPI)

**Figure 8**
Argüello Scotti and Veiga
(full width - 170 mm x 178 mm)

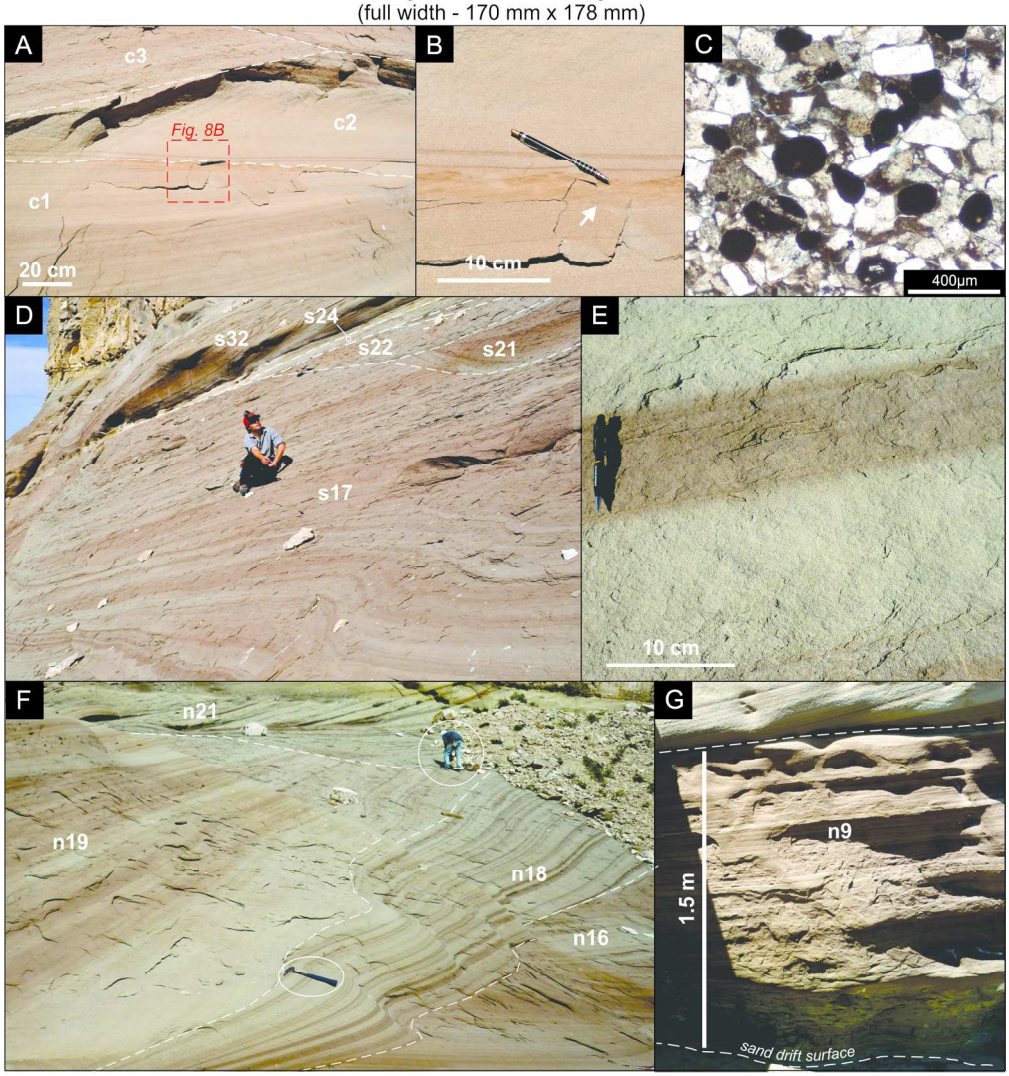


Figure 8. Details of set bodies and bounding surfaces belonging to different complexes. A) Small-scale set bodies from Complex 1, showing a stacking that forms a zigzagging arrangement of the intervening bounding surfaces (pen for scale). B) Detail of a climbing adhesion ripple stratum (lower limit marked by white arrow) found at the top of the C1 set body. Climbing translatent strata dip to the left and therefore climb in the opposite direction. C) Thin section of a sample taken from Complex 1 (location on Fig. 6B) showing the abundance of clasts of opaque minerals. D) Large-scale trough-shaped set body from Complex 2. Towards the top of the picture, very small-scale set bodies also from Complex 2 are grouped within a concave upwards bounding surface. E) Interval dominated by wind-ripple lamination, highlighted by reddish colour, between massive-looking amalgamated grainflow intervals. This is referred to as wind-ripple/grainflow couplets in the text, which are the most common form of aeolian stratification type distribution in the study section (repeated in Figs 8D, 8F). D) Large-scale wedge-shaped set bodies (n18-n19) from Complex 2. G) Wind-ripple lamination dominated lower sector of a wedge-shaped set body from Complex 2.

170x189mm (300 x 300 DPI)

**Figure 9**
Argüello Scotti and Veiga
(170 mm x 110 mm)

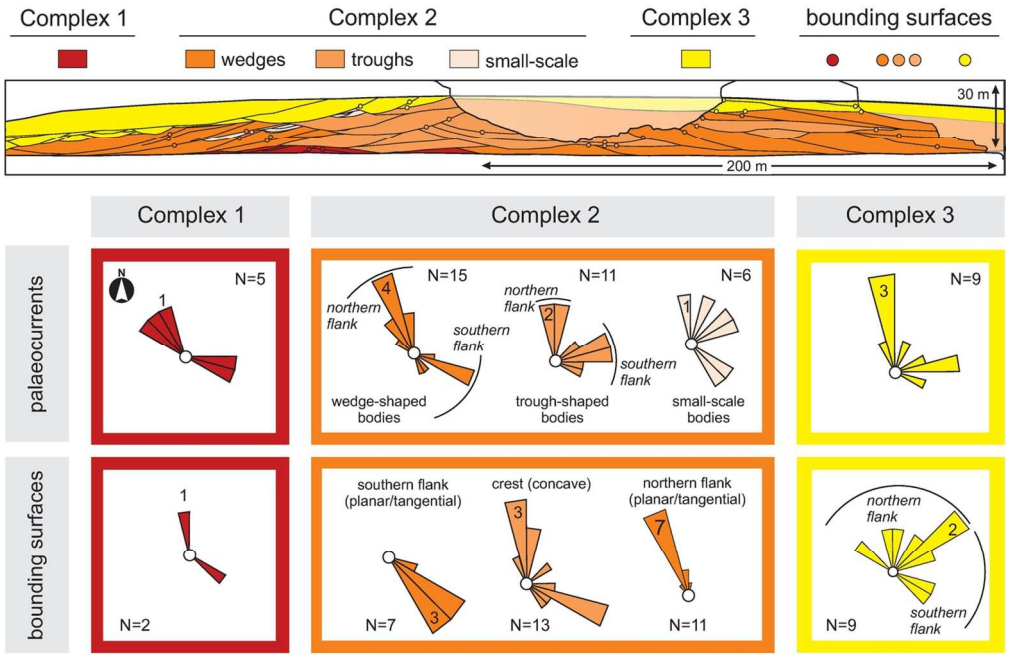


Figure 9. Palaeocurrent (averaged cross-stratification values for each set body) and bounding surface dip-azimuth distribution, arranged by complex. Panel a-a' is shown as well, indicating not only the different architectural complexes but also the different set body types within Complex 2. Palaeocurrents of Complex 2 are arranged by large-scale and very-small scale set bodies, and the former between trough-shaped and wedge-shaped sets. Bounding surfaces of Complex 2 are arranged by shape and position within the section.

123x88mm (300 x 300 DPI)

**Figure 10**
Argüello Scotti and Veiga
(2/3 page - 112 mm x 142 mm or full page width)

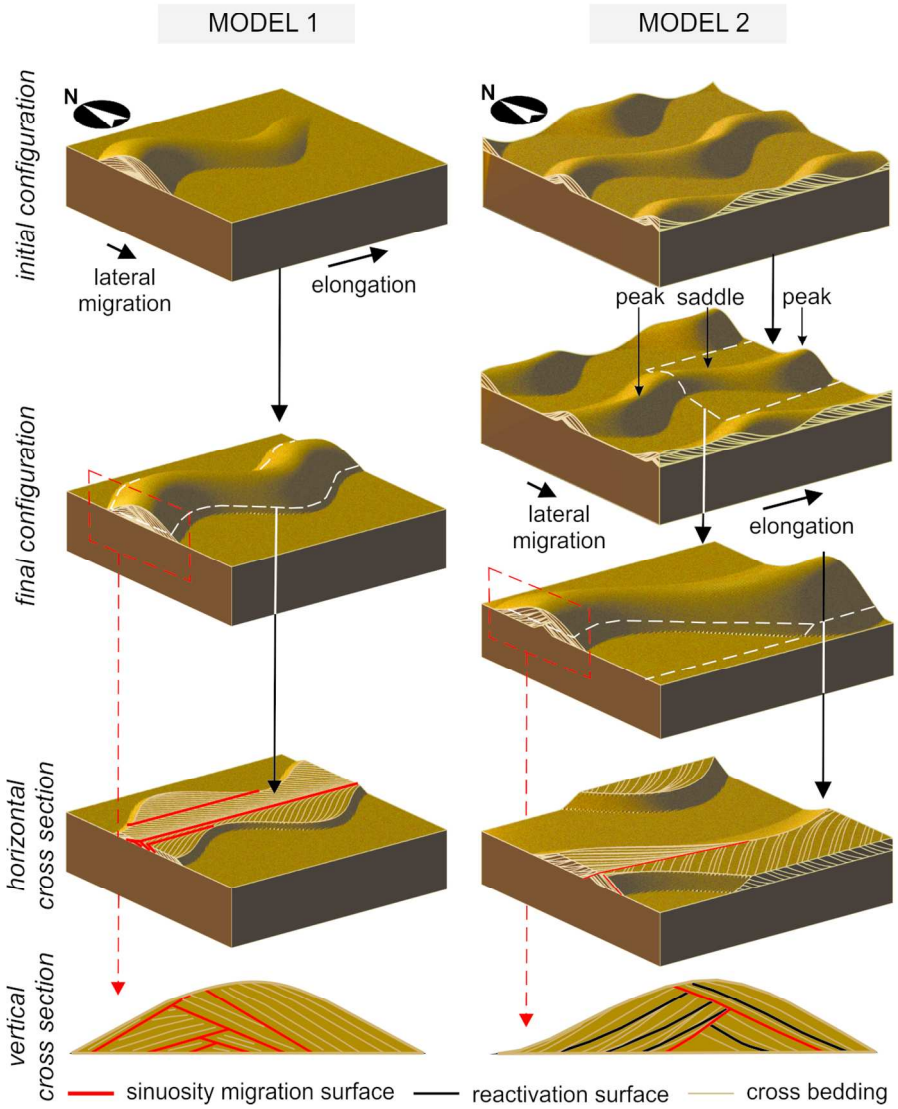


Figure 10. Deterministic models generated in BEDFORMS. Model 1 shows the resulting overall architecture from bedform development characterized by growth. Model 2 is a more detailed representation that shows the range of surface types expected in simple linear dunes. Both models show asymmetry in palaeocurrent bimodal distribution in relation to the bedform trend. The higher-hierarchy surfaces that bound cross-stratified set bodies and are formed by along-crest sinuosity migration. The lower-hierarchy surfaces that are found within cross-stratified set bodies are the result of dune profile cyclic variation.

112x148mm (300 x 300 DPI)

**Figure 11**
Argüello Scotti and Veiga
(full page width 170 mm x 154 mm)

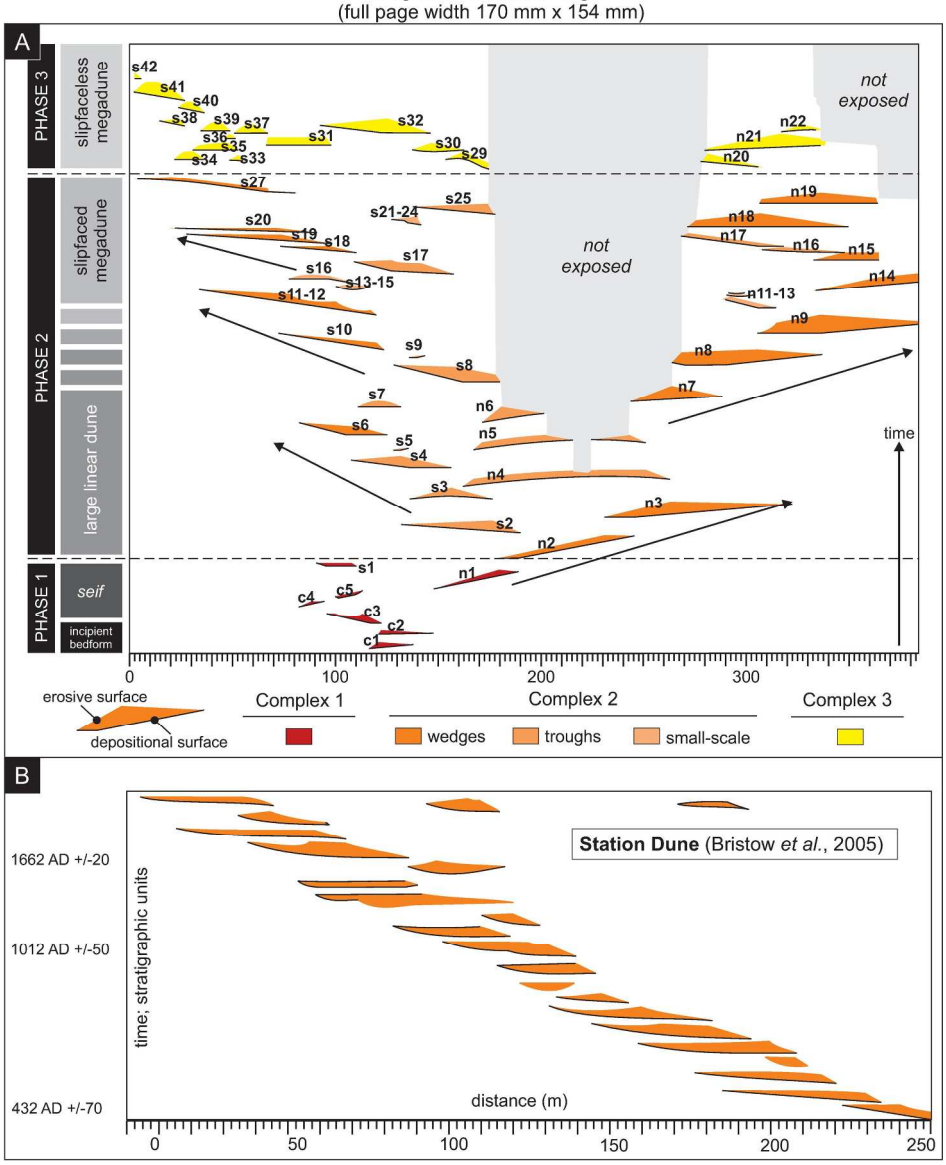


Figure 11. A) Chronostratigraphic scheme based on architectural panel a-a'. The cross-stratified set bodies are ordered in time according to a possible order or relative superposition. The set bodies have upper erosive unconformable surfaces, indicated by cross-stratification truncation, and lower depositional conformable surfaces, indicated by cross-stratification downlap and therefore time transgressive. Interpreted phases of bedform development and their associated bedform configurations are shown in time. Note the fragmentary nature of the bedform record and the gradual expansion of the preserved set bodies from a core outward. B) Chronostratigraphic scheme of Station Dune, Namibia Sand Sea, from Bristow et al. 2005. Note the shifting nature of the deposition recorded in the bedform record, strikingly different to the studied Troncoso bedform.

217x278mm (300 x 300 DPI)

**Figure 12**
Argüello Scotti and Veiga
(full page width - 170 mm x 51 mm or 2/3 of a page)

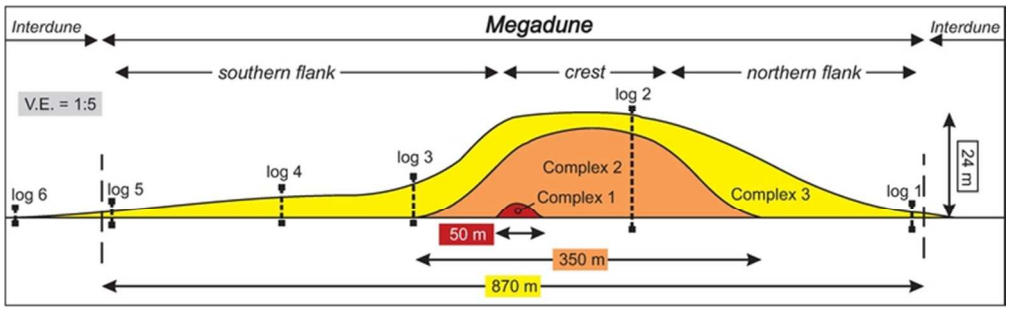


Figure 12. Architectural complex distribution, geometry and dimensions, within the preserved megadune record. Position of sedimentary logs used for control are shown as well. Preserved bedform and complex dimensions are calculated for what would be expected in a transversal section of the megadune.

66x26mm (300 x 300 DPI)

**Figure 13**
Argüello Scotti and Veiga
(2/3 page - 112 mm x 195 mm or 1 column width)

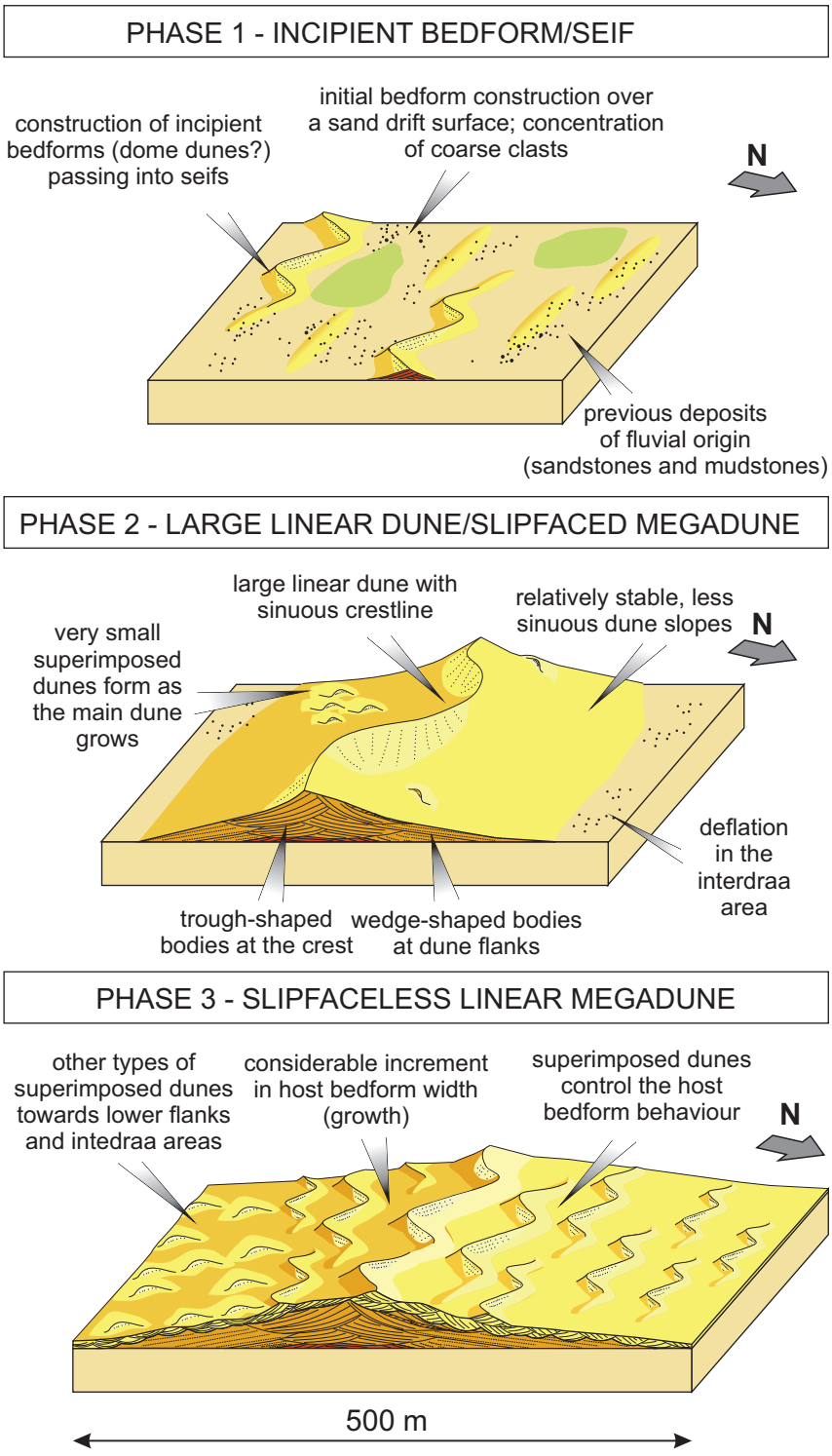

**Figure 14**
Argüello Scotti and Veiga
(2/3 page - 170 mm x 57 mm )

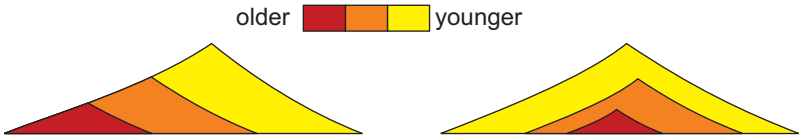


| **asymmetric** | **concentric** |
|---|---|
| one flank preserved | both flanks preserved |
| unimodal cross bedding and oblique to unimodal bounding surfaces dip-directions | bimodal (not bipolar) cross bedding and bounding surfaces dip-directions |
| sustained lateral migration | growth, accretion (accumulation), long-term longitudinal dynamics |
| conditions favorable for accumulation | conditions unfavorable for accumulation |
| asymmetric chronostratigraphic design | symmetric chronostratigraphic design |
| 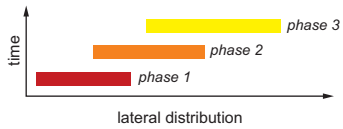 | 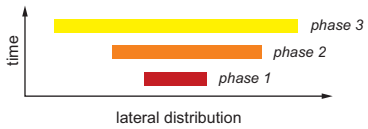 |

Table 1. Argüello Scotti and Veiga

| | **Max. thickness** | | | **Apparent Width** | | | **Geometry** |
|---|---|---|---|---|---|---|---|
| | Mean (m) | SD | N | Mean (m) | SD | N | |
| Complex 1 | 1.4 | 0.7 | 5 | 20.0 | 7.1 | 5 | wedge |
| Complex 2 (large-scale sets) | 4.4 | 1.6 | 31 | 65.6 | 29.7 | 22 | wedge + trough |
| Complex 2 (small-scale sets) | 0.9 | 0.4 | 13 | 12.4 | 9.9 | 10 | wedge + trough |
| Complex 3 | 3.1 | 1.4 | 19 | 23.2 | 13.7 | 15 | trough |

Table 2. Argüello Scotti and Veiga

**MAXIMUM THICKNESS**

| Tukey's multiple comparisons test | | | | Dunn's multiple comparisons test | | |
|---|---|---|---|---|---|---|
| | mean difference | 95% CI of difference | Significant? | | mean rank difference | Significant? |
| C2l vs. C1 | 3.036 | 1.296 to 4.78 | yes | C2l vs. C1 | 31.77 | yes |
| C2l vs. C2s | 3.542 | 2.34 to 4.74 | yes | C2l vs. C2s | 39.26 | yes |
| C2l vs. C3 | 1.288 | 0.23 to 2.34 | yes | C2l vs. C3 | 12.63 | no |
| C1 vs. C2s | 0.5065 | -1.40 to 2.42 | no | C1 vs. C2s | 7.48 | no |
| C1 vs. C3 | -1.748 | -3.57 to 0.08 | no | C1 vs. C3 | -19.14 | no |
| C2s vs. C3 | -2.254 | -3.56 to -0.95 | yes | C2s vs. C3 | -26.62 | yes |

**APPARENT WIDTH**

| Tukey's multiple comparisons test | | | | Dunn's multiple comparisons test | | |
|---|---|---|---|---|---|---|
| | mean difference | 95% CI of difference | Significant? | | mean rank difference | Significant? |
| C1 vs. C2l | -45.55 | -73.91 to -17.18 | yes | C1 vs. C2l | -21.61 | yes |
| C2l vs. C2s | 53.15 | 31.31 to 74.98 | yes | C2l vs. C2s | 30.46 | yes |
| C2l vs. C3 | 42.35 | 23.17 to 61.52 | yes | C2l vs. C3 | 20.71 | yes |
| C1 vs. C2s | 7.6 | -23.76 to 38.96 | no | C1 vs. C2s | 8.85 | no |
| C1 vs. C3 | -3.2 | -32.77 to 26.37 | no | C1 vs. C3 | -0.9 | no |
| C2s vs. C3 | -10.8 | -34.18 to 12.58 | no | C2l vs. C3 | -9.75 | no |

Table 3. Argüello Scotti and Veiga

| **Cross-bedded set body type (geometry)** | **C2 large wedges** | **C2 large troughs** |
|---|---|---|
| section location | flanks | centre |
| basal bounding surface | tangential/planar | concave upwards |
| paleocurrent distribution | obtuse bimodal | acute bimodal |
| aeolian stratification types | couplets gradually passing to wind ripple abundant/dominated | couplets abruptly passing to wind ripple abundant/dominated |
| dip angle downwards reduction | gradual | abrupt |
| dip direction variability (strength vector) | narrow (S=0,006; N=10) | wide (S=0,070; N=9) |
| interpretation | stable plinths and flanks | mobile crests |